CORA Cork Open Research Archive
Cartlann Taighde Oscailte Chorcaí

Title	A sphingosine kinase 2-mimicking TAT-peptide protects neurons against ischemia-reperfusion injury by activating BNIP3-mediated mitophagy
Authors	Chen, Jia-Li;Wang, Xin-Xin;Chen, Lei;Tang, Jie;Xia, Yun-Fei;Qian, Ke;Qin, Zheng-Hong;Waeber, Christian;Sheng, Rui
Publication date	2020-09-20
Original Citation	Chen, J.-L., Wang, X.-X., Chen, L., Tang, J., Xia, Y.-F., Qian, K., Qin, Z.-H., Waeber, C. and Sheng, R. (2020) 'A sphingosine kinase 2-mimicking TAT-peptide protects neurons against ischemia-reperfusion injury by activating BNIP3-mediated mitophagy', Neuropharmacology, 181, 108326 (14pp). https://doi.org/10.1016/j.neuropharm.2020.108326
Type of publication	Article (peer-reviewed)
Link to publisher's version	10.1016/j.neuropharm.2020.108326
Rights	© 2020, Elsevier Ltd. All rights reserved. This manuscript version is made available under the CC BY-NC-ND 4.0 license. - https://creativecommons.org/licenses/by-nc-nd/4.0/
Download date	2026-11-16 11:53:31
Item downloaded from	https://hdl.handle.net/10468/10657



UCC
University College Cork, Ireland
Coláiste na hOllscoile Corcaigh

A Sphingosine Kinase 2-mimicking TAT-peptide protects neurons against ischemia-reperfusion injury by activating BNIP3-mediated mitophagy

Jia-Li Chen[1], Xin-Xin Wang[1], Lei Chen[1], Jie Tang[1], Yun-Fei Xia[1], Ke Qian[1], Zheng-Hong Qin[1], Christian Waeber[2,3] and Rui Sheng[1]*

[1] Department of Pharmacology and Laboratory of Aging and Nervous Diseases, Jiangsu Key laboratory of Neuropsychiatric Diseases, College of Pharmaceutical Sciences of Soochow University, Suzhou, China

[2]Department of Pharmacology and Therapeutics, University College Cork, Cork, Ireland

[3] School of Pharmacy, University College Cork, Cork, Ireland

*Corresponding author
Rui Sheng, PhD
Department of Pharmacology and Laboratory of Aging and Nervous Diseases, Soochow University School of Pharmaceutical Science, Suzhou, China
199 Ren Ai Road, Suzhou 215123
Phone Number: 86-512-65882071
Fax Number: 86-512-65882071
Email: sheng_rui@163.com

Running title: A TAT-SPK2 peptide protects against cerebral ischemia/reperfusion

Abstract

We have previously shown that sphingosine kinase 2 (SPK2) interacts with Bcl-2 via its BH3 domain, activating autophagy by inducing the dissociation of Beclin-1/Bcl-2 complexes, and that a TAT-SPK2 peptide containing the BH3 domain of SPK2 protects neurons against ischemic injury. The goals of the present study were to establish the functional significance of these findings, by testing whether TAT-SPK2 was effective in a mouse model of ischemic stroke, and to explore potential underlying mechanisms. Mice were administered with TAT-SPK2 by intraperitoneal injection before or after transient middle cerebral artery occlusion (tMCAO). Infarct volume, neurological deficit and brain water content were assessed 24 h after reperfusion. Mitophagy inhibitor Mdivi-1 and BNIP3 siRNAs were used to examine the involvement of BNIP3-dependent mitophagy in the neuroprotection of TAT-SPK2. Mitophagy was quantified by immunoblotting, immunofluorescence and electron microscopy. The interaction between TAT-SPK2 and Bcl-2, Bcl-2 and BNIP3 was detected by co-immunoprecipitation. In the tMCAO model, pre-treatment with TAT-SPK2 significantly reduced infarct volume, improved neurological function and decreased brain edema. Neuroprotection by TAT-SPK2 was still seen when the peptide was administered 3 h after reperfusion. TAT-SPK2 also significantly improved functional recovery and reduced long-term brain atrophy of the ischemic hemisphere 30 days after administration. Our studies further showed that TAT-SPK2 directly binds to Bcl-2 and disrupts Bcl-2/Beclin-1 or Bcl-2/BNIP3 complexes to induce mitophagy. These results suggest that TAT-SPK2 protects neurons against ischemia reperfusion injury by activating BNIP3-mediated mitophagy. Agents exploiting this molecular mechanism are potential candidates for the treatment of ischemic stroke.

Keywords: TAT-SPK2 peptide, sphingosine kinase 2, cerebral ischemia, mitophagy, autophagy, BNIP3

Introduction

Stroke, due to a sudden loss of blood flow to a region of the brain, is one of the main causes of death worldwide. Ischemic strokes represent 80% of all strokes, and are associated with high mortality, morbidity and recurrence (Feigin et al., 2017). Intravenous recombinant tissue plasminogen activator (tPA) is still the only specific pharmacological treatment for ischemic stroke, but narrow treatment window and risk of hemorrhagic transformation limit its use (Pena et al., 2017). Thus, it is of great urgency to develop novel therapeutic drugs for ischemic stroke.

Sphingolipids, one of the largest classes of bioactive lipids, are implicated in cell structure, metabolism and signal transduction (Bartke and Hannun, 2009). Among them, sphingosine 1- phosphate (S1P), produced by the action of sphingosine kinases (SPK1 and SPK2), regulates the proliferation, survival and migration of neurons in the central nervous system (Blondeau et al., 2007; Harada et al., 2004; Song et al., 2018). Previous work from our laboratory established that isoflurane- or hypoxic preconditioning upregulated SPK2 and activated autophagy (Sheng et al., 2014b; Yung et al., 2012). The interaction of SPK2's BH3 domains with Bcl-2 might mediate autophagy activation and ischemic tolerance by inducing the dissociation of Bcl-2/ Beclin-1 complexes., we thus designed a TAT-SPK2 peptide containing the BH3 domain of SPK2 and found that it protected neurons against oxygen glucose deprivation-induced cell death (Song et al., 2017).

The aim of this study was to determine whether TAT-SPK2 is effective in vivo in an animal model of ischemic stroke and therefore shows clinical value. We also chose to focus on BCL-2/adenovirus E1B 19 kDa interacting protein 3 (BNIP3) to explore its possible underlying mechanisms. BNIP3 is primarily localized on the mitochondrial outer membrane where it plays an important role in mitochondrial dynamics (Zhang and Ney, 2009) and mitophagy (i.e., the selective removal of mitochondria by autophagy (Ashrafi and Schwarz, 2013; Youle and Narendra, 2011)). BNIP3 is a BH3 only protein that mediates hypoxia-induced mitophagy by disrupting the interaction of Beclin-1 with Bcl-2(Bellot et al., 2009), similar to the mechanism of SPK2 mediated autophagy. Since hypoxia-induced mitophagy via BNIP3 and BNIP3L is known to underpin survival mechanisms, we thus intend to test the hypothesis that TAT-SPK2 mediates neuroprotection via activation of BNIP3-mediated mitophagy by interacting with Bcl-2.

Materials and Methods.

In vivo experimental design

ICR mice (male, 8-10 weeks old, 25–30 g) were acquired from the Center of Experimental Animals of Soochow University. Animals were kept in an environment with a 12 h light/dark cycle, with free access to food and water and controlled temperature (20-25°C) and humidity (40-70%). The Chinese national guidelines for laboratory animal care and use were followed in all animal experiments. Care and handling of animals were approved by the Ethical Committee of Soochow University. The mice were randomly allocated to different groups for short-term study and long-term study (Figure S1A). In short-term study, the peptide entry, efficacy, time window and mitophagy assay of TAT-SPK2 were studied. In the long-term study, the ischemic atrophy and neurological function were investigated. The animals that showed overly deteriorated conditions after transient middle cerebral artery occlusion (tMCAO) surgery, such as inability to move, loss of consciousness, etc. were humanely euthanized. The mice were excluded from the analysis if death occurred during surgery or within 24 hours, or if the model failed for technical reasons (blood flow during MCAO did not decrease by 90% or did not return to 85-95% of baseline during reperfusion). The final number of mice included in the analysis is the total number minus the excluded number (Table S1).

Transient middle cerebral artery occlusion model in mice

Mice were anaesthetized with 1.5% (v./v.) isoflurane in air by an animal anaesthesia ventilator system. The transient middle cerebral artery occlusion (tMCAO) model in mice was implemented as described previously, using a silicone-coated nylon (6-0) monofilament (Doccol Corporation 602356PK5Re) to occlude the right MCA (Li et al., 2016). Mice were placed on a heating blanket to keep the body temperature at 37.0 ± 0.5 °C. After 2 hours of occlusion, the filament was pulled out to restore cerebral blood flow. Blood flow reduction and recovery were documented using a laser Doppler blood flow meter (LDF ML191). Further experiments were only carried out in mice whose blood flow was reduced by 90% during MCAO and recovered to 85-95% of baseline during reperfusion. After surgery, the mice were placed in an incubator until they were fully awake and active, and were placed back into cages in an environment with fewer than five mice in each cage.

Twenty-four hours after reperfusion, the neurological scores were measured by an investigator blinded to the experimental grouping using a 0-4 scale (Zhou et al., 2016).

After scoring, the mice were euthanized by decapitation under anesthesia. Brains were quickly removed. Then the infarct volume was evaluated using 2,3,5-triphenyltetrazolium chloride (TTC) staining. The brain water content was also examined as described (Huang et al., 2018; Li et al., 2016). The detailed methods are shown in the supplemental methods.

Behavioral tests and evaluation of atrophy volume

A series of behavioral tests including beam balance test and rotarod test was conducted in a separate cohort of mice at fourteen and twenty-eight days after cerebral ischemia by two investigators blinded to the experimental grouping (Huang et al., 2018) (Li et al., 2016). The detailed methods are shown in the supplemental methods.

Ipsilateral brain atrophy was used as a measure of long-term stroke-induced structural damage. Mice were euthanized after behavioral testing and perfused with PBS followed by 4% paraformaldehyde. Brains were photographed before being cut into five 2mm-thick slices; images of these slices were acquired with a scanner. The brain atrophy area in each slice was quantified using Image J (Schneider et al., 2012) and calculated using the formula: atrophy volume = (area of contralateral side – area of ipsilateral side) / whole contralateral hemisphere area ×100%.

Electron microscopy

Six hours after drug administration, adult male ICR mice weighing 25–30 g were sacrificed and perfused with PBS followed by 2.5% glutaraldehyde. The parietal cortex was dissected, post-fixed with 2.5% glutaraldehyde overnight, incubated in 1% osmium tetroxide, dehydrated in acetone and embedded in epoxy resin. Blocks were sectioned on an ultramicrotome (100 nm), stained with uranyl acetate and lead citrate, and observed under an electron microscope (JEOL JEM-1230) (Sheng et al., 2010). At least 15 cortical neurons were randomly selected from each sample to observe the double-membrane vacuole structures or vacuole structures engulfing mitochondria and partially degraded mitochondria (Sheng et al., 2014a).

Toxicology assessment

In the acute toxicity study, normal mice were administered intraperitoneally with a single dose of 80 mg/kg TAT-SPK2 (20 times the highest therapeutic dose) or TAT-L219A, and were monitored for 7 days. In the subacute toxicity study, normal mice received vehicle or TAT-SPK2 (4 mg/kg/day, intraperitoneal injection) for 2 weeks (Shen et al., 2015). The detailed methods are shown in the supplemental methods.

In vitro oxygen glucose deprivation and reoxygenation model

The experimental design of the in vitro studies is summarized in Figure S1B. Mouse hippocampal neuronal HT22 cells (Shanghai Institute of Cell Biology) were cultured in Dulbecco's modified Eagle's medium (DMEM, Gibco) supplemented with 10% fetal bovine serum (FBS, Gibco), 100 U/ml penicillin, 100 U/ml streptomycin at 37°C in 5% CO_2/95% air. The oxygen-glucose deprivation and reoxygenation (OGD/R) were performed as described previously (Cao et al., 2007). HT22 cells were incubated with HEPES balanced salt solution (HBSS: NaCl 140 mM, KCl 3.5 mM, $MgSO_4$ 12 mM, $CaCl_2$ 1.7 mM, $NaHCO_3$ 5 mM, KH_2PO_4 0.4 mM, HEPES 10 mM; pH 7.2-7.4) and placed in a chamber (Billups-Rothenberg MC-101) filled with 95% N_2 / 5% CO_2 at 37 °C. Six hours later, the HBSS was replaced with complete medium and the cells were cultured under normal condition (Sheng et al., 2012).

Cell viability assay

Cell viability was assessed using Cell Counting Kit-8 (CCK-8, Dojindo Laboratories). Cells were cultured in 96-well plates at a density of 1×10^5 cells/ well. Each well was incubated with 10μl CCK-8 medium for 2 h at 37°C. The optical density at 450 nm was measured using a plate reader (ELX 800, Bio-Tek).

Drug treatment

The TAT-SPK2 peptide (YGRKKRRQRRRGGSGDGLLYEVLNGLLDRPD) and its negative control TAT-L219A (YGRKKRRQRRRGGSGDGLLYEVANGLLDRPD) were synthesized by Chinese Peptide Company (purity 95%, Hangzhou, China) as previously described (Song et al., 2017).

For *in vivo* studies, TAT-SPK2 (1-4 mg/kg), TAT-L219A (4 mg/kg) or edaravone (3 mg/kg, positive neuroprotective control; China National Medicines Guorui Pharmaceutical Co. Ltd., Huainan, China) were dissolved in 0.9% normal saline and administered intraperitoneally (1ml/100g body weight) 1h before ischemia or at the indicated time after reperfusion. Mice were administered intraperitoneally with 8.5 μM/kg mitochondrial division inhibitor-1 (Mdivi-1,Tocris Cookson Ltd., Bristol, UK) at the beginning of reperfusion (Shen et al., 2017). Mdivi-1 was first dissolved in DMSO to prepare a 100 mM stock solution, and then diluted with normal saline to a final concentration of 0.85 mM (1 ml/100g body weight, the final DMSO concentration=0.84%). Control mice were treated with the same volume of vehicle.

For *in vitro* studies, TAT-SPK2 or TAT-L219A were dissolved in double-distilled water and then diluted as needed using complete medium. HT22 cells were incubated with 10μM TAT-SPK2 or TAT-L219A for 1-6 h. In cell viability assay, cells were

incubated with the peptides 1 h before and during OGD. Cells were then treated with 25 μM Mdivi-1 (the final DMSO concentration=0.025%) for 12 h following OGD. Control cells were treated with the same volume of vehicle.

siRNA

Small interfering RNAs specific to BNIP3 (siRNA 1, sense: 5'-GGACGAA-GUAGCUCCAAGATT-3', antisense: 5'-UCUUGGAGCUACUUCGUCCTT-3'; siRNA 2, sense: 5'-GAAGAGAAGUUGAAAGUAUTT-3', antisense: 5'-AUACU-UUCAACUUCUCUUCTT-3') and a non-silencing control siRNA (negative control, NC) were synthesized by Genepharma (Shanghai, China). BNIP3 siRNAs (40 nM) were transfected into HT22 cells using lipofectamine 2000 (Invitrogen). The efficacy of BNIP3 knockdown was assessed using Western blotting (Zhang et al., 2015).

Western blot analysis

The ipsilateral cortex, striatum and hippocampus were dissected out, homogenized and lysed with a buffer containing 150 mM NaCl, 10 mM Tris-HCl, pH 7.4, 1% sodium deoxycholate, 1% Triton X-100, 5mM EDTA, 10% SDS and 2% Protease Inhibitor Cocktail Tablets (Roche, 04693132001). Cells were washed twice with ice cold PBS and lysed in the same buffer. An aliquot of 30–50 μg protein from each sample was separated with SDS-PAGE and transferred to a nitrocellulose membrane, which was then incubated with 5% non-fat milk for 1 h. The levels of Bcl-2 (1:100; Santa Cruz sc-7382; RRID: AB_626736), Beclin-1 (1:1000, Santa Cruz sc-11427; RRID: AB_2064465), BNIP3 (1:1000; Cell Signaling Technology CST3769; RRID: AB_2259284), P62 (1:1000; Cell Signaling Technology CST5114S; RRID: AB_10624872), LC3 (1:1000; NOVUS NB600-1384; RRID: AB_669581), DRP1 (1:1000; Santa Cruz sc-101270), Parkin (1:1000; Cell Signaling Technology CST4211S), Tom20 (1:500; Proteintech 11802-1-AP) and α-tubulin (1:10000, Sigma-Aldrich T6074) was measured with Western blotting. The membranes were incubated with secondary antibodies (1:20000; LI-COR Biosciences, IRDye 800CW Donkey anti-Mouse 926–32212; RRID: AB_621847; IRDye 800CW Donkey anti-Rabbit 926–32213; RRID: AB_621848) and visualized by the Odyssey infrared imaging system (LI-COR Bioscience). The blots were analyzed using Image J, using β-actin (1:10000; Sigma A5441; RRID: AB_476744) to normalize for loading differences.

Immunofluorescence

Cells were fixed with 4% paraformaldehyde for 15min and incubated with 0.1% Triton X-100 for 10 min. Cells were then blocked with 1% BSA for 1h, and incubated with

primary antibodies against LC3 (1:500; NOVUS NB600-1384) and COXIV (1:500; CST 11967) at 4°C overnight. Then cells were incubated with anti-mouse IgG (H+L) secondary antibody, DyLight 488 (1:500; Invitrogen) and anti-rabbit IgG secondary antibody, Dylight 594 (1:1000; Invitrogen) for 3 h. Nuclei were counterstained with DAPI (1:10000; Sigma D9564) for 15 min. Fluorescence images were captured using a laser confocal microscope (ZEISS LSM710). At least 30 cells were randomly selected and observed in each group, and then the overlap coefficient was analyzed using Image J. The immunofluorescence was performed in three independent cultures.

Mitochondria isolation

Mitochondrial and cytoplasmic fractions were extracted using a commercial mitochondria isolation kit (Beyotime, C3606). Briefly, 50-100 mg of cortex were resuspended with ten volumes of solution A and then homogenized with a Kimble glass homogenizer on ice. The homogenate was centrifuged at 600 g for 5 min and then the resulting supernatant was further centrifuged at 11000 g for 10 min. The final supernatant and precipitation were cytoplasm and mitochondria respectively.

Mitochondrial function assay

The intracellular ATP level was measured using a commercial ATP assay kit (Beyotime, S0026) according to the manufacturer's protocol. Tetramethylrhodamine (TMRM) was a kind of cell-permeable dye used for analyzing mitochondrial membrane potential dynamics of living cells (Lampert et al., 2019; Li et al., 2018). Live cells were incubated with 100nM TMRM (Invitrogen I34361, 100nM) and Hoechst 33258 (Invitrogen H3569, 1μg/ml) for 30 min at 37°C. Images were captured using a fluorescence microscope system (Olympus IX73) and fluorescence intensity was quantified using Image J software.

Co-immunoprecipitation

The N-terminals of TAT-SPK2 and TAT-L219A were conjugated to biotin (Chinese Peptide Company, purity 95%). Approximately 1×10^7 cells were treated with biotinylated peptides (10 μM, 1h) and lysed in a buffer (150 mM NaCl, 50mM Tris-HCl, pH 7.4, 0.05% sodium deoxycholate, 1% NP40 and 2% Protease Inhibitor Cocktail Tablets). Then the protein concentration of each group was quantified with BCA assay. One milligram of protein from each group was incubated with M-280 streptavidin Dynabeads (Invitrogen, 11205D). The immunoprecipitates were separated with SDS-PAGE and then measured using anti-Bcl-2 antibody (Santa Cruz sc-7382) (Shoji-Kawata et al., 2013).

To examine the effect of TAT-SPK2 on the interaction between Bcl-2 and Beclin-1or BNIP3, cells were lysed in the buffer described above. The lysates were precleaned with protein A/G magnetic beads (Bimake, B23202) for 1h, and then incubated with antibody against Bcl-2 (Santa Cruz sc-7382) or IgG (normal mouse IgG, Santa Cruz sc-2025) overnight. Lysates were mixed with protein A/G magnetic beads for 6h after eluting the unbound antibody. The immunoprecipitates were separated by SDS-PAGE. Beclin-1 (Santa Cruz sc-11427) or BNIP3 (CST CST3769) was examined using Western blotting.

Statistical analysis

Data are expressed as mean ± SD unless noted otherwise. Differences between two groups were determined with unpaired two-tailed Student's t-test, while one-way or two-way repeated ANOVA was used to analyze more than two groups. When significant, omnibus tests were followed by Newman-Keuls test or Bonferroni test as post-hoc analysis. Post-hoc analysis was run only if there was no significant variance inhomogeneity. Neurological deficit score was compared using non-parametric statistics (Kruskal-Wallis test) and Dunn's test was used for post-hoc analysis. In all analyses, P values of < 0.05 were considered statistically significant.

Results

TAT-SPK2 peptide reduced ischemic injury in mouse tMCAO model.

Our previous finding showed that a TAT-SPK2 peptide designed from the BH3 domain of SPK2 protected primary neurons and HT22 neuronal cells against OGD/R injury (Song et al., 2017). Our goal was now to test the hypothesis that TAT-SPK2 is effective in vivo, in particular in an animal model of ischemic stroke. By imaging the brain tissue with Alexa Fluor 488-streptavidin conjugate, we demonstrated that biotin-TAT-SPK2 penetrates the blood brain barrier and enters the brain 6h after intraperitoneal injection (Figure S2). We next examined the efficacy of TAT-SPK2 in a mouse tMCAO model. To assess specificity, the effect of a TAT-L219A peptide composed of the BH3 domain of L219A-mutated SPK2 was also examined as a negative control (Song et al., 2017). We chose edaravone (Lei et al., 2014; Shichinohe et al., 2004) as a positive control because this small-molecular weight reactive oxygen scavenger is approved for the specific management of ischemic stroke in Japan (Jin et al., 2017). Many animal studies also use edaravone as a positive drug for the treatment of ischemic stroke (Wu et al., 2012; Zhai et al., 2013). And the dosage of edaravone (3mg/kg i.p.) used in this study

was based on literatures (Shichinohe et al., 2004; Zhang et al., 2005). The dose of TAT-SPK2 in cerebral ischemia model was determined based on preliminary experiments. Our preliminary results showed that 2mg/kg and 4mg/kg of TAT-SPK2 intraperitoneal administration could effectively reduce the infarct volume in a mouse tMCAO model (data not shown). We thus set the dose of TAT-SPK2 as 1, 2, 4mg/kg. Mice were intraperitoneally administered with TAT-SPK2 (1, 2, 4 mg/kg), TAT-L219A (4 mg/kg) or edaravone (3 mg/kg) 1 h before the ischemia. The neurological deficit and brain infarct volume were assessed 24h after reperfusion. TAT-SPK2 (1, 2 and 4 mg/kg) dose-dependently reduced the infarct volume from 57.9% ± 3.7% in the tMCAO+vehicle group, to 49.7% ± 7.2%, 41.9% ± 11.2% and 34.2% ± 8.3% respectively, while TAT-L219A failed to show any protection (55.1% ± 7.0%). TAT-SPK2 caused the largest reduction in infarct volume at 4 mg/kg and this effect was similar to that of 3 mg/kg edaravone (Figure 1A). TAT-SPK2 also restored the neurological deficit at 4mg/kg (Figure 1B) and decreased the brain water content at 1 - 4mg/kg (Figure 1C), consistent with the effects on infarct volume.

To establish a more clinically relevant therapeutic window, TAT-SPK2 (4 mg/kg) was intraperitoneally administered at reperfusion, or 1, 2, 3 or 4 h thereafter. With infarct volume at 24 hours as an outcome measure, TAT-SPK2 was effective when administered up to 3 hours after reperfusion (Figure 2A). However, a significant effect on neurological deficits was only observed when TAT-SPK2 was administered at reperfusion or 1 hour after reperfusion (Figure 2B). Interestingly, a significant effect of TAT-SPK2 on brain water content was seen at all administration time points, including 4 hours after reperfusion (Figure 2C), likely due to the lower variability of this outcome measure. Taken together, these results indicate that TAT-SPK2 could be neuroprotective after transient ischemic stroke when administered up to 3 hours after reperfusion.

To confirm that the neuroprotective effects of 4 mg/kg TAT-SPK2 (administered at reperfusion) extended beyond 24 hours, we investigated its long-term effects in mice subjected to ischemia/reperfusion injury (Huang et al., 2018; Qin et al., 2017). We assessed the behavioral recovery 14 and 28 days after tMCAO. At 14 days after tMCAO, the mice showed obvious neurological deficit. Compared with the sham group, the mice passed the balance beam with a longer time (Figure 3B) and fell off the rotarod easily (Figure 3C). The neurological behavior of mice recovered at 28 days after tMCAO, but there is still a certain degree of behavioral impairment, which may

be due to the severity of the tMCAO model and behavioral evaluation system in this study (Huang et al., 2018; Li et al., 2016; Qin et al., 2017) . At both 14 and 28 days after tMCAO, TAT-SPK2 shortened the time to get through the balance beam (Figure 3B) and extended the time to fall off the rotarod (Figure 3C) compared to vehicle-treated mice. The shrinkage/atrophy of the ischemic hemisphere was assessed 30 days after ischemia/reperfusion. Compared to vehicle-treated mice, TAT-SPK2 markedly decreased the atrophy volume from 49.6% ± 6.9% to 26.5% ± 6.3% (Figure 3A). These data suggested the TAT-SPK2-mediated reduction of ischemic hemisphere atrophy was accompanied with long-term functional recovery in mouse tMCAO model.

We conducted a preliminary toxicological evaluation of the TAT-SPK2 peptide. None of the 12 normal mice administered intraperitoneally with a single dose of 80 mg/kg TAT-SPK2 (20 times the highest therapeutic dose) or TAT-L219A (6 mice per group) died within 7 days. The body weight (Figure S3A), food and water intake, breathing, excretion, and behavior of the mice did not change significantly during one week of follow-up. There was no significant difference among TAT-SPK2, TAT-L219A and control group in the levels of blood biomarkers reflecting organ toxicity including creatinine (Figure S3B) for kidney, glutamic pyruvic transaminase (GPT, alanine aminotransferase, ALT, Figure S3C) and glutamic oxalacetic transaminase (GOT, aspartate aminotransferase, AST, Figure S3D) for liver, and lactate dehydrogenase 1 (LDH1, Figure S3E) for heart damage. HE-staining of organs including heart, lung liver, kidney, spleen and testis also showed no obvious histopathological changes (Figure S3F). These results in a small cohort of mice suggest that a single 20 times the highest therapeutic dose of TAT-SPK2 peptide displayed no overt organ toxicity in mice.

We also performed a long-term chronic safety evaluation with TAT-SPK2 at therapeutic dose (4 mg/kg). Daily 4 mg/kg TAT-SPK2 was well tolerated in adult mice during a two-week treatment (6 mice per group). During the period of observation, there were no visual difference between mice in terms of feeding and water intake, breathing, excretion and daily behavior (Data not shown). Compared with vehicle controls, mice had normal weight gain (Figure 4A) and organ weight indices of liver, spleen and kidney (Figure 4B-D). There was also no statistical difference between TAT-SPK2 and control in the levels of blood biomarkers including creatinine (Figure 4E), ALT (Figure 4F), AST (Figure 4G) and LDH1 (Figure 4H). No observable histopathological changes in HE-staining of sections from heart, lung liver, kidney, spleen and testis was found

either (Figure 4I). These results further suggest that daily 4 mg/kg TAT-SPK2 peptide during a two-week treatment displayed no overt organ toxicity in mice.

TAT-SPK2 peptide induced mitophagy *in vivo* and *in vitro*

To investigate whether autophagy or mitophagy underlies TAT-SPK2-mediated protection against ischemia/reperfusion, we assessed the autophagic markers LC3 and P62 in cortex, hippocampus and striatum 1, 3, 6, 12 and 24 h after TAT-peptide administration to control mice. TAT-SPK2 (T-S), but not TAT-L219A (T-L) significantly upregulated LC3II/β-actin ratio in cortex (Figure 5A) and hippocampus (Figure S2A) after 6 h treatment, whereas LC3II/β-actin was markedly increased in striatum from 6 h-24 h (Figure S4A). P62 was significantly down-regulated in the three brain regions at 6 h (Figure 5B, Figure S4B) of TAT-SPK2 treatment.

We then used electron microscopy to evaluate autophagosome formation in cortical neurons. In the cortical neurons of mice treated with vehicle or TAT-L219A, the organelles and nuclei seemed normal and healthy. The mitochondria had complete and clear double membrane and crista structures. Six hours after TAT-SPK2 treatment, the organelles and nuclei in neurons also appeared normal without significant damage, but increased number of double-membrane structures containing mitochondria and partially degraded mitochondria was found in TAT-SPK2 group compared with control or TAT-L219A group, suggesting possible mitophagy induction after TAT-SPK2 treatment (Figure 5D). The mitochondrial recruitment of DRP1, PINK1/Parkin is crucial for mediating mitophagy activation (Chen and Dorn, 2013; Feng et al., 2018a; Rana et al., 2017). We thus investigated the distribution of DRP1, Parkin and P62 in the mitochondrial and cytoplasmic fractions of mouse cortex after TAT-SPK2 treatment. The results showed that six hours after the administration of TAT-SPK2, compared with the vehicle or TAT-L219A treatment group, more DRP1 and Parkin were recruited in the mitochondria, accompanied by more degradation of mitochondrial P62 (Figure 5E). These data further support the activation of mitophagy by TAT-SPK2.

Our previous work established that one-hour treatment with TAT-SPK2, but not with TAT-L219A, could activate autophagy in HT22 neuronal cells (Song et al., 2017). In the present study, we further evaluated mitophagy in HT22 cells 1 h after TAT-SPK2 administration using double-staining immunofluorescence microscopy. Mitochondria and autophagosomes were visualized with mitochondrial marker COXIV and with LC3, respectively. TAT-SPK2 increased the overlap between COXIV-stained mitochondria and LC3-stained autophagosomes in HT22 cells compared with control

and TAT-L219A groups (Figure 5F), supporting the notion that TAT-SPK2 administration was associated with increased mitophagy. Taken together, our data indicate that TAT-SPK2 peptide activates mitophagy both *in vivo* and *in vitro*.

Inhibition of mitophagy blocks the neuroprotection of TAT-SPK2 peptide

To elucidate the role of mitophagy in TAT-SPK2-mediated neuroprotection, we tested the effects of a mitophagy inhibitor in *in vitro* and *in vivo* models of cerebral ischemia/reperfusion. Mdivi-1 is a specific inhibitor of dynamin-related protein 1 (DRP1), a mitochondrial fission protein (Tanaka and Youle, 2008) used in many recent studies as an inhibitor of mitophagy (Cassidy-Stone et al., 2008; Mizumura et al., 2014; Pi et al., 2013; Zhang et al., 2013). Mitophagy usually target small and round mitochondria. When Mdivi-1 inhibits mitochondrial fission, the mitochondria that have not undergone fission cannot be engulfed by phagophores, the precursors to autophagosomes; hence, Mdivi-1 can indirectly inhibit mitophagy.

HT22 cells were incubated with TAT-SPK2 or TAT-L219A for 1 h. Cells were then subjected to 6 h of OGD and exposed to Mdivi-1 immediately after re-oxygenation. As shown in the results, Mdivi-1 significantly reduced the protective effect of TAT-SPK2 (Figure 6A).

Similar results were obtained in vivo. Mice were administered with 4 mg/kg TAT-SPK2 at the onset of ischemia, and then subjected to tMCAO. Mdivi-1 (3 mg/kg), administered intraperitoneally at the onset of reperfusion, partially abolished the neuroprotective effects of TAT-SPK2, which was reflected in the increased infarct volumes and worse neurological scores (Figure 6B-D). Overall, these data offer support for the hypothesis that mitophagy is involved in TAT-SPK2-mediated neuroprotection against cerebral ischemia.

BNIP3 is involved in the neuroprotection conferred by TAT-SPK2 peptide

BNIP3 plays a key role in hypoxia-induced mitophagy (Bellot et al., 2009). BNIP3 binds to LC3 on the autophagosome and induces autophagic clearance of both endoplasmic reticulum (“ER-phagy”) and mitochondria (mitophagy) (Hanna et al., 2012). However, it is unclear whether BNIP3 is required for TAT-SPK2-mediated mitophagy. Our in vivo studies showed that TAT-SPK2 treatment significantly increased BNIP3 protein levels at 6 h in the cortex (Figure 5C), striatum and hippocampus (Figure S5). Consistently, in HT22 cell cultures, BNIP3 protein levels increased 1-6 h after treatment with TAT-SPK2 compared with the control or TAT-L219A groups (Figure 7A).

We next investigated whether BNIP3 contributes to TAT-SPK2-induced mitophagy and neuroprotection. BNIP3 was knocked down by two siRNAs, which efficiently reduced BNIP3 expression in HT22 cells compared to the negative control (Figure 7B). Notably, both BNIP3 siRNAs significantly reversed TAT-SPK2-induced overlap between COXIV and LC3 labeling (Figure 7C), indicating that BNIP3 is required for TAT-SPK2-induced mitophagy activation. In addition, knockdown of BNIP3 effectively abolished TAT-SPK2-mediated protection (Figure 7D). Role of autophagy/mitophagy activation in ischemic stroke is controversial (Feng et al., 2017). Moderate mitophagy may help to maintain mitochondrial function, while excess mitophagy may lead to mitochondrial dysfunction (Ashrafi and Schwarz, 2013; Palikaras et al., 2018). To further investigate the effect of TAT-SPK2-mediated mitophagy on mitochondrial function, we evaluated mitochondrial function by assessing ATP level and mitochondrial membrane potential. The results showed that ATP level (Figure 7E) and mitochondrial membrane potential assessed by TMRM staining (Figure 7F) were significantly reduced in neuronal cells treated with OGD/R, while TAT-SPK2 resumed the ATP level and mitochondrial membrane potential compared to OGD/R group. Importantly, BNIP3 knockdown eliminated the protective effect of TAT-SPK2 on mitochondrial function, indicating that TAT-SPK2 may help to restore mitochondrial function via BNIP3-mediated mitophagy. Overall, these data suggest that BNIP3-dependent mitophagy is involved in TAT-SPK2-induced neuroprotection against cerebral ischemia.

TAT-SPK2 peptide interacts with Bcl-2 and disrupts the BNIP3/Bcl-2 and Beclin-1/Bcl-2 complex

We have previously shown that SPK2 interacts with Bcl-2 via its BH3 domain to induce the dissociation of Beclin-1/Bcl-2 complexes (Song et al., 2017). We thus performed biochemical analyses with biotin-conjugated TAT-SPK2 to test the hypothesis that our TAT-SPK2 peptide, designed based on the BH3 domain of SPK2, interacts with Bcl-2 as well. Endogenous Bcl-2 immunoprecipitated with the biotin-TAT-SPK2 but not with biotin-TAT-L219A (Figure 8A). As expected, TAT-SPK2 treatment markedly decreased the co-immunoprecipitation of Beclin1/Bcl-2 (Figure 8B-C). BNIP3 is known to interact with Bcl-2 directly via its BH3 domain to regulate mitophagy (Bellot et al., 2009; Maiuri et al., 2007; Mazure and Pouyssegur, 2009; Song et al., 2017; Zhang et al., 2008) . We thus further tested the co-immunoprecipitation of BNIP3 and Bcl-2 in HT22 cells after TAT-SPK2 treatment. TAT-SPK2 markedly reduced the amount of

BNIP3 co-immunoprecipitated with Bcl-2 compared with TAT-L219A and the control (Figure 8D-E). Overall, these findings confirm that TAT-SPK2 interacts with Bcl-2 to induce the dissociation of BNIP3/Bcl-2 or Beclin-1/Bcl-2 complexes.

Discussion

SPK2 seems to play a role in cerebral preconditioning, but the cell types and mechanisms underlying this effect has not been fully characterized (Song et al., 2018; Wacker et al., 2012; Wacker et al., 2009; Yung et al., 2012). An SPK2-dependent mechanism is also involved in the neuroprotection against cerebral ischemia (Pfeilschifter et al., 2011). Our previous finding showed that isoflurane- or hypoxia-induced preconditioning could increase SPK2 expression to activate autophagy and mediate ischemic tolerance (Sheng et al., 2014b). SPK2 activates autophagy by dissociating Bcl-2/ Beclin-1 complex via interaction with the BH3 domain of Bcl-2. Accordingly, we designed an SPK2-derived TAT-peptide containing the BH3 domain of SPK2 (TAT-SPK2) (Song et al., 2017). In the present study, we sought to investigate whether TAT-SPK2 is effective in a mouse model of ischemic stroke. We found that TAT-SPK2 penetrates the mouse brain after intraperitoneal injection. In a mouse tMCAO model, TAT-SPK2 reduced infarct volume and decreased brain water content in a dose-dependent manner, while it improved neurological deficit at the highest dose. TAT-SPK2 also significantly improved functional recovery and reduced long-term brain atrophy of the ischemic hemisphere 30 days after administration. A single dose of 80 mg/kg of TAT-SPK2 (20-fold therapeutic dose) or daily 4 mg/kg treatment in healthy adult mice for two weeks was well tolerated and showed no overt toxicity. All these data suggest that TAT-SPK2 peptide may prove as a candidate of therapeutic agent against ischemic stroke.

During cerebral ischemia/reperfusion, moderate induction of mitophagy is an effective strategy to reduce neuronal damage and to improve stroke outcome in ischemic stroke (Liu et al., 2013; Shen et al., 2017). PARK2-mediated mitophagy during reperfusion can effectively clear damaged mitochondria, which render the brains resistance to ischemic injury (Zhang et al., 2013) (Zhang et al., 2014) (Shen et al., 2017). Mitochondria are dynamic organelles constantly undergoing fission, fusion, biogenesis and selective degradation (Anne Stetler et al., 2013) and interfering with their dynamics may have an important effect on cell survival. Silencing or inhibition of DRP1 (dynamin-related protein 1), a key mediator of mitochondrial fission, increases the

vulnerability of neurons to oxygen/glucose deprivation or global ischemia and prevents ischemia‑induced mitophagy (Zuo et al., 2016). In the present study, we used immunoblotting and immunofluorescence with autophagy/mitophagy markers, and electron microscopy to confirm that TAT-SPK2 could induce mitophagy in neurons in vivo and in vitro, and that mitophagy is involved in TAT-SPK2-mediated neuroprotection against cerebral ischemia.

Mitophagy is regulated by at least two pathways, including Parkin-dependent mitophagy and receptor-mediated mitophagy (Bravo-San Pedro et al., 2017). BNIP3 is one of the receptor-related factors that mediates mitophagy (Georgakopoulos et al., 2017). BNIP3 interacts with LC3 to tether damaged mitochondria to autophagosomes through its LC3 interacting region (LIR) motifs towards the cytosol, initiating the process of mitophagy (Rikka et al., 2011; Shi et al., 2014). In natural killer cells, BNIP3 and BNIP3L play essential roles in the clearance of dysfunctional mitochondria and mitochondria-associated reactive oxygen species (ROS) to promote cell survival (O'Sullivan et al., 2015). BNIP3L knockout mice show impaired mitophagy, larger infarct volumes and worse neurological deficit following transient middle cerebral artery occlusion (Yuan et al., 2017). The feasibility of inducing cell protection via drug-induced upregulation of BNIP3-mediated mitophagy was recently documented in a study of the effects of mitochonic acid 5 on tumor necrosis factor α-induced apoptosis of microglial BV-2 cells (Lei et al., 2018). We have now demonstrated that another agent, TAT-SPK2, elicits neuroprotection against ischemia/reperfusion through activation of BNIP3-mediated mitophagy.

Indeed, role of autophagy/mitophagy activation in ischemic stroke is controversial (Feng et al., 2017). Basic mitophagy is neuroprotective, whereas excessive mitophagy is detrimental (Ashrafi and Schwarz, 2013; Palikaras et al., 2018). Moderate mitophagy to clear ischemia/ reperfusion- injured mitochondria may improve mitochondrial function such as balance of ROS and ATP generation and inhibition of apoptosis, thus helping to protect cerebral ischemia/reperfusion injury (Green et al., 2011; Tang et al., 2016; Zhang et al., 2013). However, other studies have shown excessive mitophagy may exacerbate cerebral ischemic injury. ROS and reactive nitrogen species (RNS) are crucial players in activating mitophagy (Nakamura and Lipton, 2020; Xiao et al., 2017). Peroxynitrite is a kind of RNS that promotes the recruitment of DRP1 to damaged mitochondria and induces excessive mitophagy, thereby aggravating the brain damage

after cerebral ischemia (Feng et al., 2018a). Naringin, a natural antioxidant, can inhibit peroxynitrite-mediated mitophagy to protect against ischemia/reperfusion injury (Feng et al., 2018b). Therefore, the role of mitophagy in ischemic stroke may be a double-edged sword. Following factors should be considered in the studies on autophagy/mitophagy in ischemic stroke to determine whether autophagy/mitophagy is beneficial or detrimental: (1) Protocols for administration of autophagy regulators including administration time points, routes and doses, etc.; (2) Specificity of autophagy regulators; (3) Animal models of cerebral ischemia with or without reperfusion (Feng et al., 2017). To support the induction of mitophagy would be benefit for ischemic brains in the study, we thus investigated mitochondrial function after TAT-SPK2 administration. ATP levels and mitochondrial membrane potential decreased significantly in neurons undergoing ischemia/reperfusion, which can be restored by TAT-SPK2. However, knockdown of BNIP3 eliminated the protective effect of TAT-SPK2 on mitochondrial function, suggesting that TAT-SPK2 -induced mitophagy via BNIP3 may help to restore mitochondrial function, thereby preventing ischemia/reperfusion injury.

Our previous results demonstrated that SPK2 directly interacts with Bcl-2 through its putative BH3 domain, and competes with Beclin1 in Beclin1/ Bcl-2 complex to activate autophagy (Sheng et al., 2014b; Song et al., 2017). We thus hypothesized that a TAT-SPK2 peptide designed based on the BH3 domain of SPK2 would also interact with Bcl-2 to break the Beclin-1/Bcl-2 complex. As expected, TAT-SPK2 immunoprecipitated with endogenous Bcl-2 and decreased the co-immunoprecipitation of Beclin1 and Bcl-2. BNIP3 is known to heterodimerize with Bcl-2 through its BH3 domain (Bellot et al., 2009). Interestingly, TAT-SPK2 but not TAT-L219A, also reduced the co-immunoprecipitation between Bcl-2 and BNIP3. These data suggest that TAT-SPK2 may directly bind to Bcl-2 and disrupt the Bcl-2/BNIP3 complex to activate mitophagy.

Although this study indicates that TAT-SPK2 protects neurons against ischemia/ reperfusion injury by activating BNIP3-mediated mitophagy, it should be noted that there are still some limitations in this work. First, although we have shown that Mdivi-1 partially abolished the neuroprotection of TAT-SPK2 in cerebral ischemia via inhibition of mitophagy, we did not study the effect of Mdivi-1 on its own on cerebral ischemia. Nevertheless, it is worth noting that some studies have shown that Mdivi-1 is able to ameliorate cerebral ischemic injury (Cui et al., 2016; Zhao et al., 2014) (Feng

et al., 2018a), suggesting that Mdivi-1 does not have a detrimental effect on ischemic brains. Moreover, the pharmacokinetics parameters (e.g., half-life or plasma clearance of TAT-SPK2) have not been explored in the study. Another potential issue with this study is the high mortality in long term study following tMCAO, which decreased the statistical power of the study, and might have led to the selection of mice with less severe ischemia-reperfusion injury or those affected by an undefined pro-survival factor. Although TAT-SPK2 did seem to improve the survival rate of tMCAO mice, this effect did not reach statistical significance (data not shown), possibly because the peptide was administered only once in long term study. The effect of multiple administration of TAT-SPK2 on the long-term survival curve and neurological function of tMCAO mice needs further investigation. Furthermore, our data showed that TAT-SPK2 induced significant neuroprotection when administered up to 3 h after reperfusion. Its treatment window might be comparable to that of rtPA (4.5h after reperfusion) (Demaerschalk et al., 2016). For future clinical application, whether there is an interaction between rtPA and TAT-SPK2 and whether TAT-SPK2 enhances the therapeutic effect of rtPA or alleviates the hemorrhagic transformation of rtPA will be the research direction for further investigation in the follow-up research.

In summary, the present study demonstrated that TAT-SPK2 peptide could directly bind to Bcl-2 and disrupt the Beclin-1/ Bcl-2 complex and BNIP3/ Bcl-2 complex to induce mitophagy. Thus TAT-SPK2 may protect neurons against ischemia/reperfusion injury by activating BNIP3-mediated mitophagy. TAT-SPK2 peptide may become a potential candidate for the treatment of ischemic stroke.

Author contributions

R.S. conceived and directed the study. J.L.C., X.X.W., L.C., and J.T. performed the experiments. J.L.C., Y.F.X. and K.Q. collected, analysed and interpreted the data. J.L.C. wrote the manuscript. Z.H.Q., C.W. and R.S. revised the manuscript. All authors discussed the results and commented on the manuscript.

Declaration of Interest

The author declares no conflict of interest

Acknowledgements

This work was supported by grants from the National Natural Science Foundation of China (No. 81973315, 81673421 and 81373402) and Jiangsu Key Laboratory of Neuropsychiatric Diseases (BM2013003).

References

Anne Stetler, R., Leak, R. K., Gao, Y., Chen, J., 2013. The dynamics of the mitochondrial organelle as a potential therapeutic target. J Cereb Blood Flow Metab 33, 22-32.

Ashrafi, G., Schwarz, T. L., 2013. The pathways of mitophagy for quality control and clearance of mitochondria. Cell Death Differ 20, 31-42.

Bartke, N., Hannun, Y. A., 2009. Bioactive sphingolipids: metabolism and function. Journal Of Lipid Research 50 Suppl, S91-96.

Bellot, G., Garcia-Medina, R., Gounon, P., Chiche, J., Roux, D., Pouyssegur, J., Mazure, N. M., 2009. Hypoxia-induced autophagy is mediated through hypoxia-inducible factor induction of BNIP3 and BNIP3L via their BH3 domains. Molecular And Cellular Biology 29, 2570-2581.

Blondeau, N., Lai, Y., Tyndall, S., Popolo, M., Topalkara, K., Pru, J. K., Zhang, L., Kim, H., Liao, J. K., Ding, K., Waeber, C., 2007. Distribution of sphingosine kinase activity and mRNA in rodent brain. J Neurochem 103, 509-517.

Bravo-San Pedro, J. M., Kroemer, G., Galluzzi, L., 2017. Autophagy and Mitophagy in Cardiovascular Disease. Circ Res 120, 1812-1824.

Cao, G., Xing, J., Xiao, X., Liou, A. K., Gao, Y., Yin, X. M., Clark, R. S., Graham, S. H., Chen, J., 2007. Critical role of calpain I in mitochondrial release of apoptosis-inducing factor in ischemic neuronal injury. J Neurosci 27, 9278-9293.

Cassidy-Stone, A., Chipuk, J. E., Ingerman, E., Song, C., Yoo, C., Kuwana, T., Kurth, M. J., Shaw, J. T., Hinshaw, J. E., Green, D. R., Nunnari, J., 2008. Chemical inhibition of the mitochondrial division dynamin reveals its role in Bax/Bak-dependent mitochondrial outer membrane permeabilization. Dev Cell 14, 193-204.

Chen, Y., Dorn, G. W., 2nd, 2013. PINK1-phosphorylated mitofusin 2 is a Parkin receptor for culling damaged mitochondria. Science 340, 471-475.

Cui, M., Ding, H., Chen, F., Zhao, Y., Yang, Q., Dong, Q., 2016. Mdivi-1 Protects Against Ischemic Brain Injury via Elevating Extracellular Adenosine in a cAMP/CREB-CD39-Dependent Manner. Mol Neurobiol 53, 240-253.

Demaerschalk, B. M., Kleindorfer, D. O., Adeoye, O. M., Demchuk, A. M., Fugate, J. E., Grotta, J. C., Khalessi, A. A., Levy, E. I., Palesch, Y. Y., Prabhakaran, S., Saposnik, G., Saver, J. L., Smith, E. E., American Heart Association Stroke, C., Council on, E., Prevention, 2016. Scientific Rationale for the Inclusion and Exclusion Criteria for Intravenous Alteplase in Acute Ischemic Stroke: A Statement for Healthcare Professionals From the American Heart Association/American Stroke Association. Stroke 47, 581-641.

Feigin, V. L., Norrving, B., Mensah, G. A., 2017. Global Burden of Stroke. Circ Res 120, 439-448.

Feng, J., Chen, X., Guan, B., Li, C., Qiu, J., Shen, J., 2018a. Inhibition of Peroxynitrite-Induced Mitophagy Activation Attenuates Cerebral Ischemia-Reperfusion Injury. Mol Neurobiol 55, 6369-6386.

Feng, J., Chen, X., Lu, S., Li, W., Yang, D., Su, W., Wang, X., Shen, J., 2018b. Naringin Attenuates Cerebral Ischemia-Reperfusion Injury Through Inhibiting Peroxynitrite-Mediated Mitophagy Activation. Mol Neurobiol 55, 9029-9042.

Feng, J., Chen, X., Shen, J., 2017. Reactive nitrogen species as therapeutic targets for autophagy: implication for ischemic stroke. Expert Opin Ther Targets 21, 305-317.

Georgakopoulos, N. D., Wells, G., Campanella, M., 2017. The pharmacological regulation of cellular mitophagy. Nat Chem Biol 13, 136-146.

Green, D. R., Galluzzi, L., Kroemer, G., 2011. Mitochondria and the autophagy-inflammation-cell death axis in organismal aging. Science 333, 1109-1112.

Hanna, R. A., Quinsay, M. N., Orogo, A. M., Giang, K., Rikka, S., Gustafsson, A. B., 2012. Microtubule-associated protein 1 light chain 3 (LC3) interacts with Bnip3 protein to selectively remove endoplasmic reticulum and mitochondria via autophagy. J Biol Chem 287, 19094-19104.

Harada, J., Foley, M., Moskowitz, M. A., Waeber, C., 2004. Sphingosine-1-phosphate induces proliferation and morphological changes of neural progenitor cells. J Neurochem 88, 1026-1039.

Huang, Q., Sun, M., Li, M., Zhang, D., Han, F., Wu, J. C., Fukunaga, K., Chen, Z., Qin, Z. H., 2018. Combination of NAD(+) and NADPH Offers Greater Neuroprotection in Ischemic Stroke Models by Relieving Metabolic Stress. Mol Neurobiol 55, 6063-6075.

Jin, Q., Cai, Y., Li, S., Liu, H., Zhou, X., Lu, C., Gao, X., Qian, J., Zhang, J., Ju, S., Li, C., 2017. Edaravone-Encapsulated Agonistic Micelles Rescue Ischemic Brain Tissue by Tuning Blood-Brain Barrier Permeability. Theranostics 7, 884-898.

Lampert, M. A., Orogo, A. M., Najor, R. H., Hammerling, B. C., Leon, L. J., Wang, B. J., Kim, T., Sussman,

M. A., Gustafsson, A. B., 2019. BNIP3L/NIX and FUNDC1-mediated mitophagy is required for mitochondrial network remodeling during cardiac progenitor cell differentiation. Autophagy 15, 1182-1198.
Lei, Q., Tan, J., Yi, S., Wu, N., Wang, Y., Wu, H., 2018. Mitochonic acid 5 activates the MAPK-ERK-yap signaling pathways to protect mouse microglial BV-2 cells against TNFalpha-induced apoptosis via increased Bnip3-related mitophagy. Cell Mol Biol Lett 23, 14.
Lei, S., Zhang, P., Li, W., Gao, M., He, X., Zheng, J., Li, X., Wang, X., Wang, N., Zhang, J., Qi, C., Lu, H., Chen, X., Liu, Y., 2014. Pre- and posttreatment with edaravone protects CA1 hippocampus and enhances neurogenesis in the subgranular zone of dentate gyrus after transient global cerebral ischemia in rats. ASN Neuro 6.
Li, G., Yang, J., Yang, C., Zhu, M., Jin, Y., McNutt, M. A., Yin, Y., 2018. PTENalpha regulates mitophagy and maintains mitochondrial quality control. Autophagy 14, 1742-1760.
Li, M., Zhou, Z. P., Sun, M., Cao, L., Chen, J., Qin, Y. Y., Gu, J. H., Han, F., Sheng, R., Wu, J. C., Ding, Y., Qin, Z. H., 2016. Reduced Nicotinamide Adenine Dinucleotide Phosphate, a Pentose Phosphate Pathway Product, Might Be a Novel Drug Candidate for Ischemic Stroke. Stroke 47, 187-195.
Liu, K., Sun, Y., Gu, Z., Shi, N., Zhang, T., Sun, X., 2013. Mitophagy in ischaemia/reperfusion induced cerebral injury. Neurochem Res 38, 1295-1300.
Maiuri, M. C., Criollo, A., Tasdemir, E., Vicencio, J. M., Tajeddine, N., Hickman, J. A., Geneste, O., Kroemer, G., 2007. BH3-only proteins and BH3 mimetics induce autophagy by competitively disrupting the interaction between Beclin 1 and Bcl-2/Bcl-X(L). Autophagy 3, 374-376.
Mazure, N. M., Pouyssegur, J., 2009. Atypical BH3-domains of BNIP3 and BNIP3L lead to autophagy in hypoxia. Autophagy 5, 868-869.
Mizumura, K., Cloonan, S. M., Nakahira, K., Bhashyam, A. R., Cervo, M., Kitada, T., Glass, K., Owen, C. A., Mahmood, A., Washko, G. R., Hashimoto, S., Ryter, S. W., Choi, A. M., 2014. Mitophagy-dependent necroptosis contributes to the pathogenesis of COPD. J Clin Invest 124, 3987-4003.
Nakamura, T., Lipton, S. A., 2020. Nitric Oxide-Dependent Protein Post-Translational Modifications Impair Mitochondrial Function and Metabolism to Contribute to Neurodegenerative Diseases. Antioxid Redox Signal 32, 817-833.
O'Sullivan, T. E., Johnson, L. R., Kang, H. H., Sun, J. C., 2015. BNIP3- and BNIP3L-Mediated Mitophagy Promotes the Generation of Natural Killer Cell Memory. Immunity 43, 331-342.
Palikaras, K., Lionaki, E., Tavernarakis, N., 2018. Mechanisms of mitophagy in cellular homeostasis, physiology and pathology. Nat Cell Biol 20, 1013-1022.
Pena, I. D., Borlongan, C., Shen, G., Davis, W., 2017. Strategies to Extend Thrombolytic Time Window for Ischemic Stroke Treatment: An Unmet Clinical Need. J Stroke 19, 50-60.
Pfeilschifter, W., Czech-Zechmeister, B., Sujak, M., Mirceska, A., Koch, A., Rami, A., Steinmetz, H., Foerch, C., Huwiler, A., Pfeilschifter, J., 2011. Activation of sphingosine kinase 2 is an endogenous protective mechanism in cerebral ischemia. Biochemical And Biophysical Research Communications 413, 212-217.
Pi, H., Xu, S., Zhang, L., Guo, P., Li, Y., Xie, J., Tian, L., He, M., Lu, Y., Li, M., Zhang, Y., Zhong, M., Xiang, Y., Deng, L., Zhou, Z., Yu, Z., 2013. Dynamin 1-like-dependent mitochondrial fission initiates overactive mitophagy in the hepatotoxicity of cadmium. Autophagy 9, 1780-1800.
Qin, Y. Y., Li, M., Feng, X., Wang, J., Cao, L., Shen, X. K., Chen, J., Sun, M., Sheng, R., Han, F., Qin, Z. H., 2017. Combined NADPH and the NOX inhibitor apocynin provides greater anti-inflammatory and neuroprotective effects in a mouse model of stroke. Free Radic Biol Med 104, 333-345.
Rana, A., Oliveira, M. P., Khamoui, A. V., Aparicio, R., Rera, M., Rossiter, H. B., Walker, D. W., 2017. Promoting Drp1-mediated mitochondrial fission in midlife prolongs healthy lifespan of Drosophila melanogaster. Nat Commun 8, 448.
Rikka, S., Quinsay, M. N., Thomas, R. L., Kubli, D. A., Zhang, X., Murphy, A. N., Gustafsson, A. B., 2011. Bnip3 impairs mitochondrial bioenergetics and stimulates mitochondrial turnover. Cell Death Differ 18, 721-731.
Schneider, C. A., Rasband, W. S., Eliceiri, K. W., 2012. NIH Image to ImageJ: 25 years of image analysis. Nat Methods 9, 671-675.
Shen, A. Z., Li, X., Hu, W., Chen, F. H., 2015. Total flavonoids of Bidens bipinnata L. ameliorate experimental adjuvant-induced arthritis through induction of synovial apoptosis. BMC Complement Altern Med 15, 437.
Shen, Z., Zheng, Y., Wu, J., Chen, Y., Wu, X., Zhou, Y., Yuan, Y., Lu, S., Jiang, L., Qin, Z., Chen, Z., Hu, W., Zhang, X., 2017. PARK2-dependent mitophagy induced by acidic postconditioning protects against focal cerebral ischemia and extends the reperfusion window. Autophagy 13, 473-485.

Sheng, R., Liu, X. Q., Zhang, L. S., Gao, B., Han, R., Wu, Y. Q., Zhang, X. Y., Qin, Z. H., 2012. Autophagy regulates endoplasmic reticulum stress in ischemic preconditioning. Autophagy 8, 310-325.
Sheng, R., Zhang, L. S., Han, R., Liu, X. Q., Gao, B., Qin, Z. H., 2010. Autophagy activation is associated with neuroprotection in a rat model of focal cerebral ischemic preconditioning. Autophagy 6, 482-494.
Sheng, R., Zhang, T. T., Felice, V. D., Qin, T., Qin, Z. H., Smith, C. D., Sapp, E., Difiglia, M., Waeber, C., 2014a. Preconditioning stimuli induce autophagy via sphingosine kinase 2 in mouse cortical neurons. J Biol Chem 289, 20845-20857.
Sheng, R., Zhang, T. T., Felice, V. D., Qin, T., Qin, Z. H., Smith, C. D., Sapp, E., Difiglia, M., Waeber, C., 2014b. Preconditioning Stimuli Induce Autophagy via Sphingosine Kinase 2 in Mouse Cortical Neurons. Journal Of Biological Chemistry 289, 20845-20857.
Shi, R. Y., Zhu, S. H., Li, V., Gibson, S. B., Xu, X. S., Kong, J. M., 2014. BNIP3 interacting with LC3 triggers excessive mitophagy in delayed neuronal death in stroke. CNS Neurosci Ther 20, 1045-1055.
Shichinohe, H., Kuroda, S., Yasuda, H., Ishikawa, T., Iwai, M., Horiuchi, M., Iwasaki, Y., 2004. Neuroprotective effects of the free radical scavenger Edaravone (MCI-186) in mice permanent focal brain ischemia. Brain Res 1029, 200-206.
Shoji-Kawata, S., Sumpter, R., Leveno, M., Campbell, G. R., Zou, Z., Kinch, L., Wilkins, A. D., Sun, Q., Pallauf, K., MacDuff, D., Huerta, C., Virgin, H. W., Helms, J. B., Eerland, R., Tooze, S. A., Xavier, R., Lenschow, D. J., Yamamoto, A., King, D., Lichtarge, O., Grishin, N. V., Spector, S. A., Kaloyanova, D. V., Levine, B., 2013. Identification of a candidate therapeutic autophagy-inducing peptide. Nature 494, 201-206.
Song, D. D., Zhang, T. T., Chen, J. L., Xia, Y. F., Qin, Z. H., Waeber, C., Sheng, R., 2017. Sphingosine kinase 2 activates autophagy and protects neurons against ischemic injury through interaction with Bcl-2 via its putative BH3 domain. Cell Death & Disease 8, e2912.
Song, D. D., Zhou, J. H., Sheng, R., 2018. Regulation and function of sphingosine kinase 2 in diseases. Histol Histopathol 33, 433-445.
Tanaka, A., Youle, R. J., 2008. A chemical inhibitor of DRP1 uncouples mitochondrial fission and apoptosis. Mol Cell 29, 409-410.
Tang, Y. C., Tian, H. X., Yi, T., Chen, H. B., 2016. The critical roles of mitophagy in cerebral ischemia. Protein Cell 7, 699-713.
Wacker, B. K., Freie, A. B., Perfater, J. L., Gidday, J. M., 2012. Junctional protein regulation by sphingosine kinase 2 contributes to blood-brain barrier protection in hypoxic preconditioning-induced cerebral ischemic tolerance. Journal of Cerebral Blood Flow & Metabolism 32, 1014-1023.
Wacker, B. K., Park, T. S., Gidday, J. M., 2009. Hypoxic preconditioning-induced cerebral ischemic tolerance: role of microvascular sphingosine kinase 2. Stroke 40, 3342-3348.
Wu, J., Ling, J., Wang, X., Li, T., Liu, J., Lai, Y., Ji, H., Peng, S., Tian, J., Zhang, Y., 2012. Discovery of a potential anti-ischemic stroke agent: 3-pentylbenzo[c]thiophen-1(3H)-one. J Med Chem 55, 7173-7181.
Xiao, B., Goh, J. Y., Xiao, L., Xian, H., Lim, K. L., Liou, Y. C., 2017. Reactive oxygen species trigger Parkin/PINK1 pathway-dependent mitophagy by inducing mitochondrial recruitment of Parkin. J Biol Chem 292, 16697-16708.
Youle, R. J., Narendra, D. P., 2011. Mechanisms of mitophagy. Nat Rev Mol Cell Biol 12, 9-14.
Yuan, Y., Zheng, Y., Zhang, X., Chen, Y., Wu, X., Wu, J., Shen, Z., Jiang, L., Wang, L., Yang, W., Luo, J., Qin, Z., Hu, W., Chen, Z., 2017. BNIP3L/NIX-mediated mitophagy protects against ischemic brain injury independent of PARK2. Autophagy 13, 1754-1766.
Yung, L. M., Wei, Y., Qin, T., Wang, Y., Smith, C. D., Waeber, C., 2012. Sphingosine kinase 2 mediates cerebral preconditioning and protects the mouse brain against ischemic injury. Stroke 43, 199-204.
Zhai, X., Chen, X., Shi, J., Shi, D., Ye, Z., Liu, W., Li, M., Wang, Q., Kang, Z., Bi, H., Sun, X., 2013. Lactulose ameliorates cerebral ischemia-reperfusion injury in rats by inducing hydrogen by activating Nrf2 expression. Free Radic Biol Med 65, 731-741.
Zhang, H., Bosch-Marce, M., Shimoda, L. A., Tan, Y. S., Baek, J. H., Wesley, J. B., Gonzalez, F. J., Semenza, G. L., 2008. Mitochondrial autophagy is an HIF-1-dependent adaptive metabolic response to hypoxia. J Biol Chem 283, 10892-10903.
Zhang, J., Ney, P. A., 2009. Role of BNIP3 and NIX in cell death, autophagy, and mitophagy. Cell Death Differ 16, 939-946.
Zhang, N., Komine-Kobayashi, M., Tanaka, R., Liu, M., Mizuno, Y., Urabe, T., 2005. Edaravone reduces early accumulation of oxidative products and sequential inflammatory responses after transient focal ischemia in mice brain. Stroke 36, 2220-2225.
Zhang, X., Yan, H., Yuan, Y., Gao, J., Shen, Z., Cheng, Y., Shen, Y., Wang, R. R., Wang, X., Hu, W. W., Wang,

G., Chen, Z., 2013. Cerebral ischemia-reperfusion-induced autophagy protects against neuronal injury by mitochondrial clearance. Autophagy 9, 1321-1333.
Zhang, X., Yuan, Y., Jiang, L., Zhang, J., Gao, J., Shen, Z., Zheng, Y., Deng, T., Yan, H., Li, W., Hou, W. W., Lu, J., Shen, Y., Dai, H., Hu, W. W., Zhang, Z., Chen, Z., 2014. Endoplasmic reticulum stress induced by tunicamycin and thapsigargin protects against transient ischemic brain injury: Involvement of PARK2-dependent mitophagy. Autophagy 10, 1801-1813.
Zhang, X. Y., Zhang, T. T., Song, D. D., Zhou, J., Han, R., Qin, Z. H., Sheng, R., 2015. Endoplasmic reticulum chaperone GRP78 is involved in autophagy activation induced by ischemic preconditioning in neural cells. Mol Brain 8, 20.
Zhao, Y. X., Cui, M., Chen, S. F., Dong, Q., Liu, X. Y., 2014. Amelioration of ischemic mitochondrial injury and Bax-dependent outer membrane permeabilization by Mdivi-1. CNS Neurosci Ther 20, 528-538.
Zhou, J. H., Zhang, T. T., Song, D. D., Xia, Y. F., Qin, Z. H., Sheng, R., 2016. TIGAR contributes to ischemic tolerance induced by cerebral preconditioning through scavenging of reactive oxygen species and inhibition of apoptosis. Sci Rep 6, 27096.
Zuo, W., Yang, P. F., Chen, J., Zhang, Z., Chen, N. H., 2016. Drp-1, a potential therapeutic target for brain ischaemic stroke. Br J Pharmacol 173, 1665-1677.

Figure 1. TAT-SPK2 peptide reduced ischemic injury in a mouse model of transient focal cerebral ischemia. Mice were subjected to transient middle cerebral artery occlusion (tMCAO) for 2 h. TAT-SPK2 peptide (1, 2, and 4 mg/kg), TAT-L219A peptide (4 mg/kg) and edaravone (3 mg/kg) was administered intraperitoneally 1 h before the onset of ischemia respectively. (A) The infarct volume was detected with TTC staining 24 h after reperfusion. The quantitative analysis showed that TAT-SPK2 decreased ischemia/reperfusion-induced infarction. The neurological deficit (**B**) and water content (**C**) was also examined at 24 h after reperfusion. n=9-12 animals in each group. The neurological deficit scores are shown as median while other data are shown as mean ± SD. * P<0.05, ** P< 0.01, *** P<0.001 compared with the vehicle group.

Figure 2. The therapeutic window of the neuroprotection of TAT-SPK2 peptide on tMCAO-induced ischemic injury. Mice were subjected to tMCAO for 2 h and were intraperitoneally administered with TAT-SPK2 peptide (4 mg/kg) at 0, 1, 2, 3, and 4 h after reperfusion. The effects of TAT-SPK2 peptide on infarct volume (A), neurological deficit (B) and water content (C) were detected at 24 h after reperfusion. n=8-11 animals in each group. The neurological deficit scores are shown as median while other data are shown as mean ± SD. * P<0.05, ** P< 0.01, *** P<0.001 compared with the vehicle group.

Figure 3. Long-term effects of TAT-SPK2 on brain atrophy and functional recovery in tMCAO mice. Mice were subjected to tMCAO for 2 h and were intraperitoneally administered with TAT-SPK2 (4 mg/kg) at the onset of reperfusion. Mice were kept for 14 and 28 post-stroke days and then behavior tests were performed. (A) Representative images and quantification showed that TAT-SPK2 reduced brain shrinkage of the ischemic hemisphere (right) 30 days after tMCAO. (B-C) Effects of TAT-SPK2 on the beam balance (B) and rotarod test(C). n=6 animals in each group. Data are shown as mean ± SD. * P<0.05, ** P< 0.01, *** P<0.001.

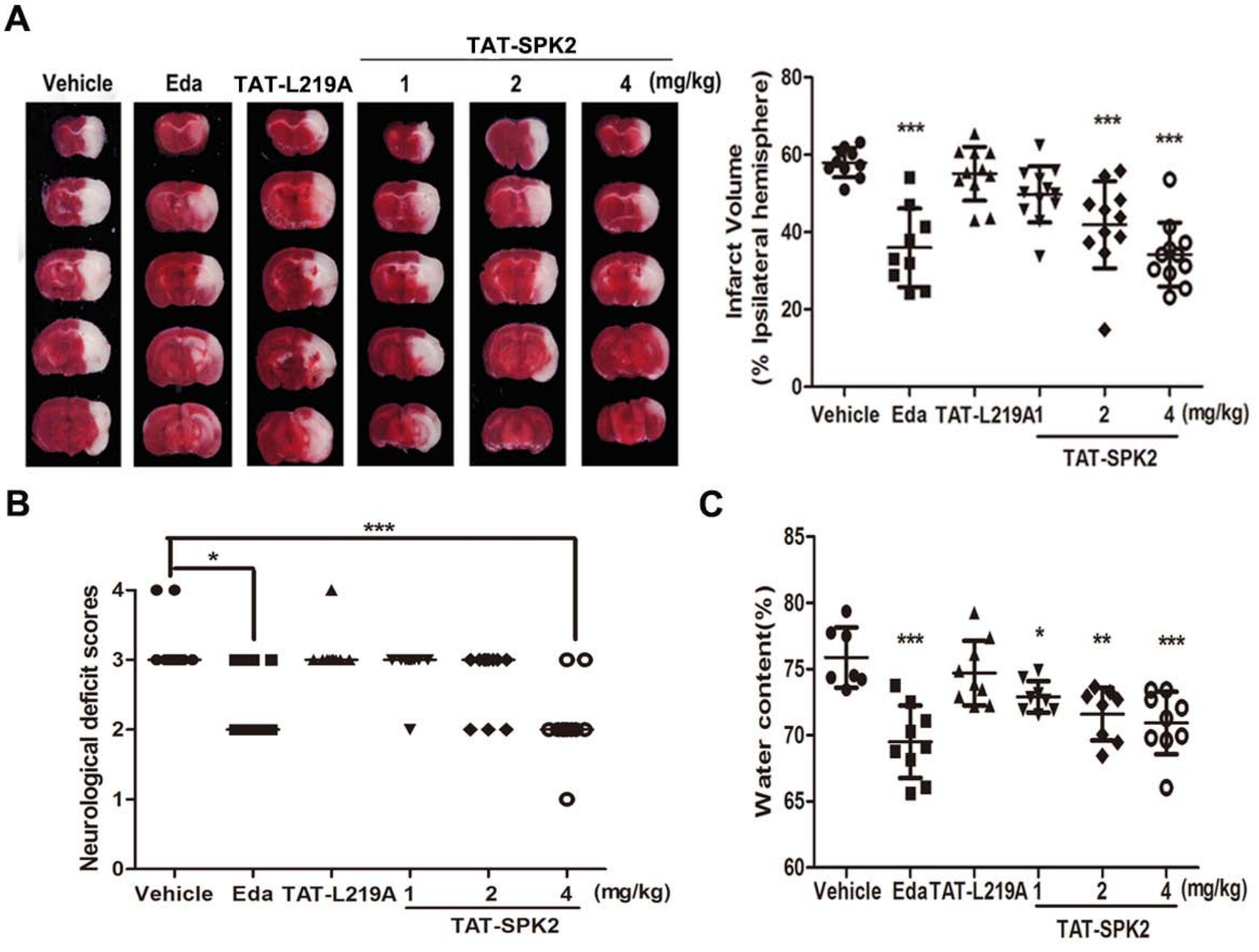
Figure 4. Daily TAT-SPK2 treatment displayed no overt toxicity in mice. Mice were treated with either vehicle or TAT-SPK2 (4 mg/kg/day, intraperitoneal injection) for 2 weeks. The effects of TAT-SPK2 on body (A), liver (B), spleen (C) and kidney (D) weights were assessed. Some representative objective blood biomarkers of organs toxicity were tested including creatinine (E) for kidney, glutamic pyruvic transaminase (GPT, alanine aminotransferase, ALT) (F) and glutamic oxalacetic transaminase (GOT, aspartate aminotransferase, AST) (G) for liver, and lactate dehydrogenase 1 (LDH1) for heart (H). (I) Organs including liver, spleen, kidney, testis, heart and lung were dissected and stained with haematoxylin and eosin. Representative images are shown. Scale bar = 50 μm. n=6 mice in each group. Data are shown as mean ± SD.

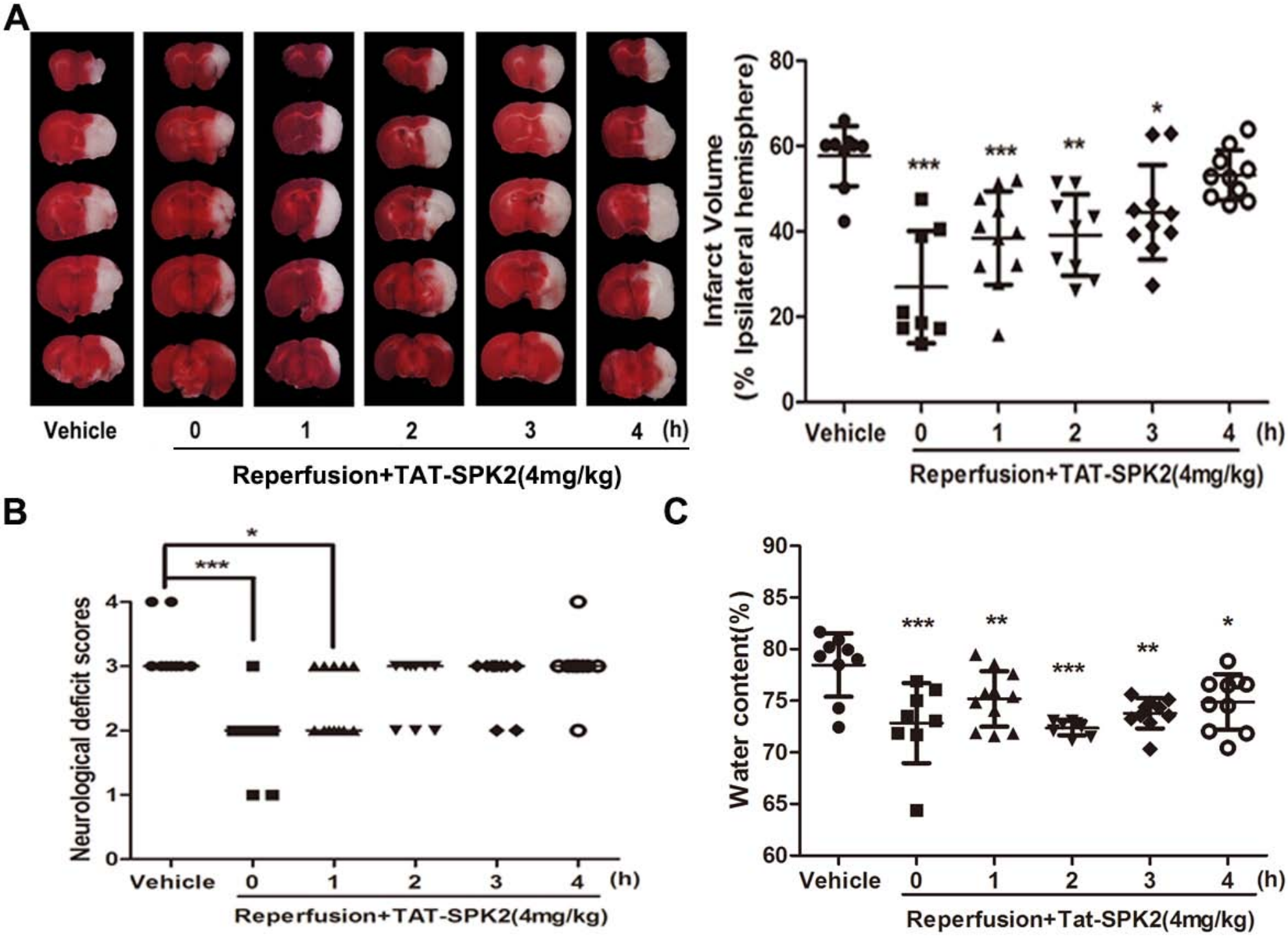
Figure 5. TAT-SPK2 induced mitophagy *in vivo* and *in vitro*. Mice were treated with TAT-SPK2 or TAT-L219A (4 mg/kg, intraperitoneally). Cortex was dissected 1, 3, 6, 12, and 24 h after administration. The levels of LC3 (A) and P62 (B) and BNIP3 (C) were determined with Western blotting. β-actin levels were used as loading control. n=6 mice in each group. T-L: TAT-L219A; T-S: TAT-SPK2. (D) Electron microscopic images show increased number of double-membrane vacuolar structure containing mitochondria and partially degraded mitochondria in the TAT-SPK2-treated group. Scale bar = 1 μm. N: nucleus. Arrows indicate autophagosomes with engulfed mitochondria or mitochondria being wrapped by endoplasmic reticulum, which are enlarged in the rightmost insets. (E) DRP1, P62 and Parkin in cytosolic and mitochondrial fractions of cortex from mice treated with TAT-SPK2 or TAT-L219A (4 mg/kg, intraperitoneal). Cyto: cytosolic fraction; Mito: mitochondrial fraction. Tom20 is a mitochondrial marker amd α-tubulin is a cytosolic marker. n=6 mice in each group. (F) TAT-SPK2 increased the colocalization of LC3 and COXIV in HT22 cells. HT22 cells were treated with 10 μM TAT-SPK2 or TAT-L219A for 1 h. The rightmost column shows enlarged cells taken from the boxed area. Scale bar=10 μm. *n*=3 independent experiments. The histogram represents the Manders overlap coefficient of LC3 and COXIV in HT22 cells. Data ware shown as mean ± SD. * $P<0.05$, ** $P< 0.01$, *** $P<0.001$ compared with the control group.

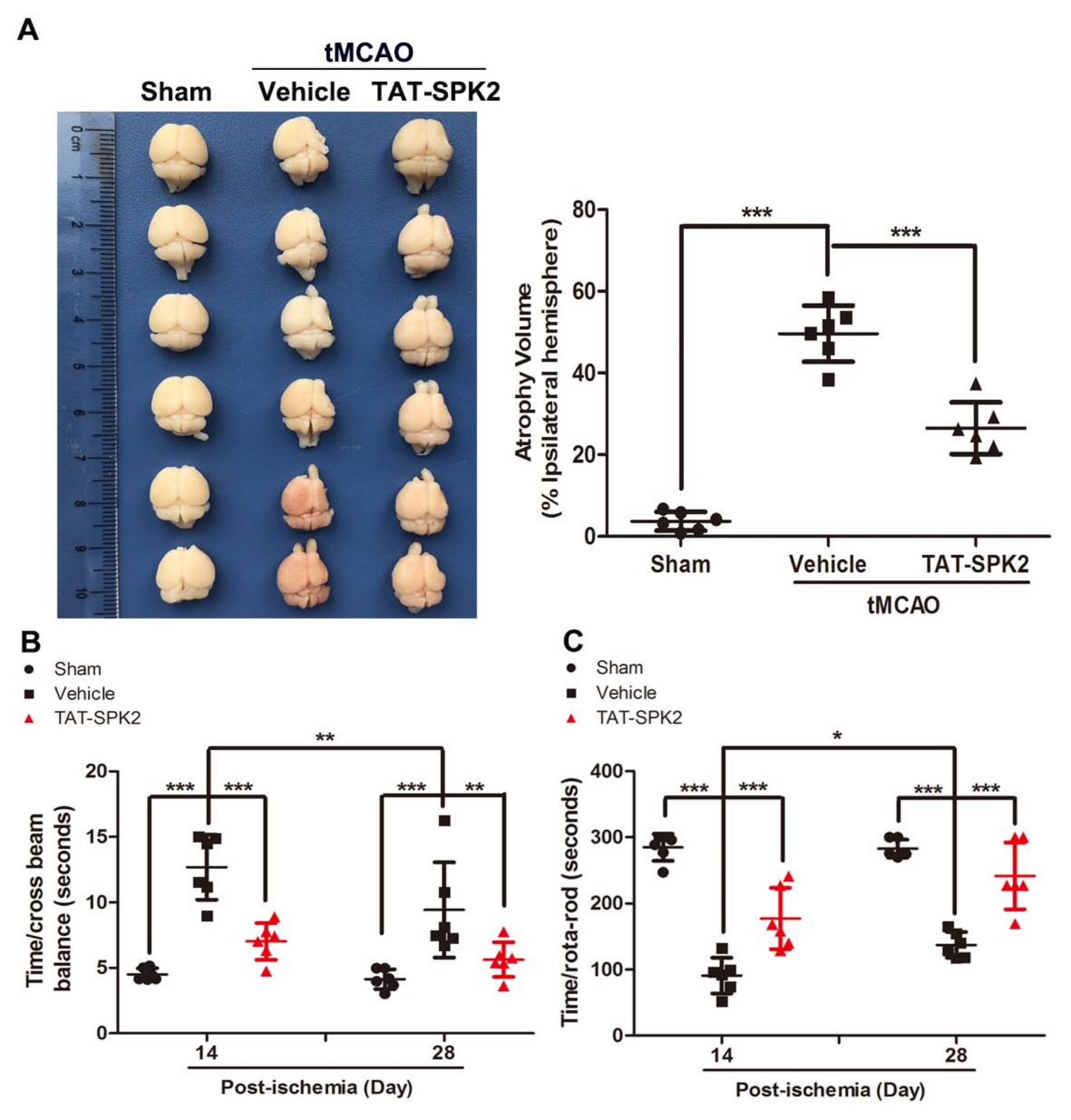
Figure 6. Inhibition of mitophagy with Mdivi-1 blocked the neuroprotection of TAT-SPK2 peptide *in vitro* and *in vivo*. (A) HT22 cells were treated with TAT-SPK2 or TAT-L219A peptide at 10 μM for 1h, and then were subjected to 6 h of oxygen glucose deprivation (OGD). Cells were treated with Mdivi-1 (25 μM) immediately after reperfusion. The cell viability was assessed by cell counting kit-8 assay. *n*=3 independent experiments. (B-D) Mice were administered with 4 mg/kg TAT-SPK2 peptide 1 h before ischemia, and then subjected to tMCAO for 2 h. Mdivi-1 (8.5 μM/kg, intraperitoneally) was applied at the onset of reperfusion. The infarct volume and neurological deficit was detected at 24 h after reperfusion. n=9-13 animals in each group. The neurological deficit scores were presented as median while other data were presented as mean ± SD. * P<0.05, ** P< 0.01, *** P<0.001.

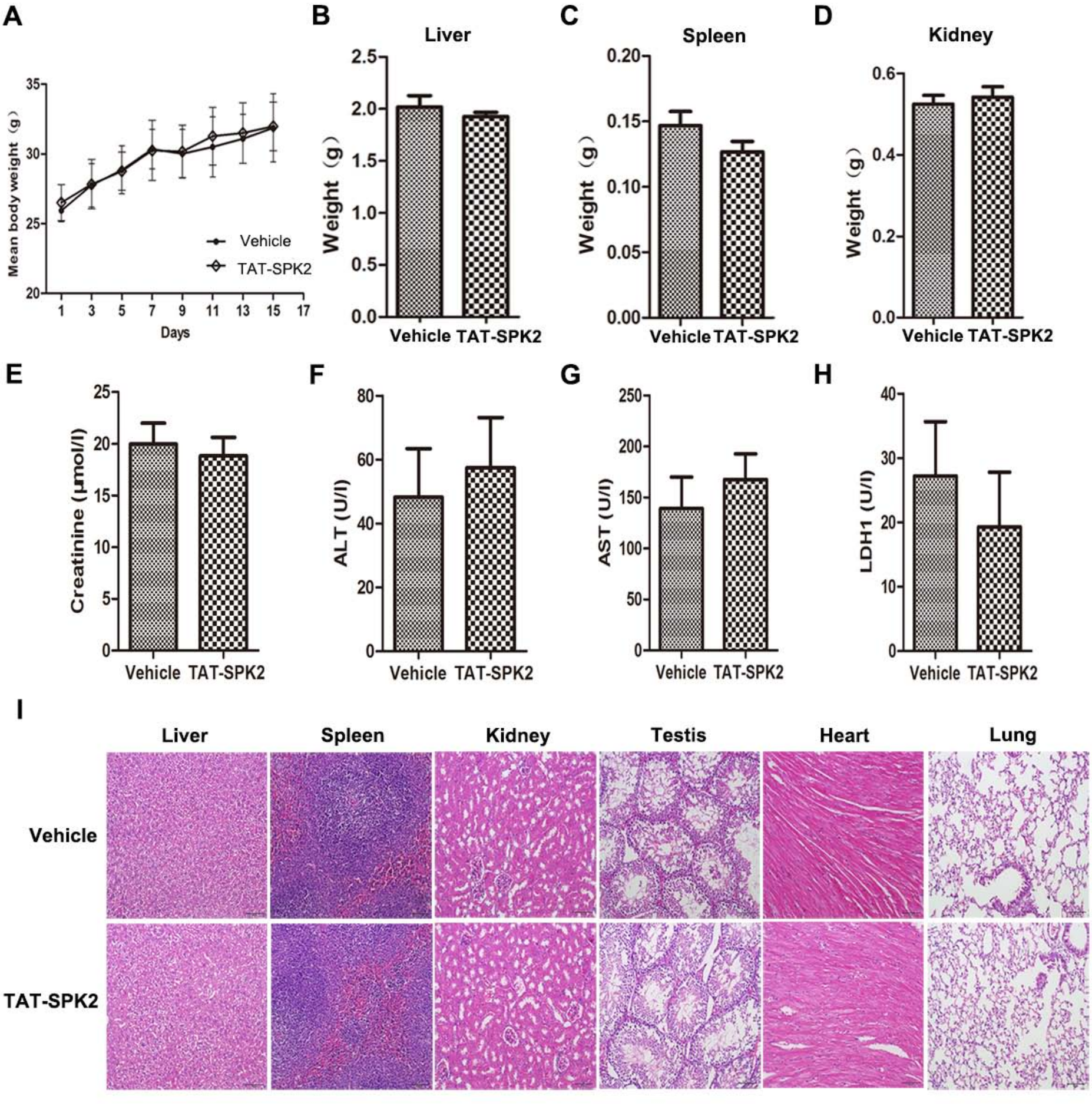
Figure 7. BNIP3 was involved in the neuroprotection conferred by TAT-SPK2 peptide. (A) TAT-SPK2 but not TAT-L219A upregulated BNIP3 *in vitro*. HT22 cells were treated with 10 μM TAT-SPK2 or TAT-L219A peptide for indicated time. Then the cells were harvested and subjected to Western blot analysis. β-actin levels were used as loading control. (B) HT22 cells were transfected with BNIP3 siRNA using lipofectamine 2000. BNIP3 was measured with Western blotting. NC: negative control. (C) BNIP3 knockdown abolished TAT-SPK2 peptide-induced mitophagy activation. Cells were treated with 10 μM TAT-SPK2 for 1 h. Rightmost insets show enlarged cells taken from the boxed area. Scale bar=10 μm. The histogram represents the Manders overlap coefficient of LC3 and COXIV in HT22 cells. (D) BNIP3 knockdown abolished TAT-SPK2-induced protection. 72 h after transfection, cells were treated with TAT-SPK2 or TAT-L219A at the indicated concentration for 1 h, and then exposed to OGD/reperfusion. The cell viability was assessed by cell counting kit-8 assay. (E-F) BNIP3 knockdown canceled the protective effect of TAT-SPK2 peptide on mitochondrial function represented by ATP levels (E) and TMRM fluorescence (F) in HT22 cells. Scale bar=100 μm. *n*=3 independent experiments. Data were presented as mean ± SD. * P<0.05, ** P< 0.01, *** P<0.001 compared with the control group.

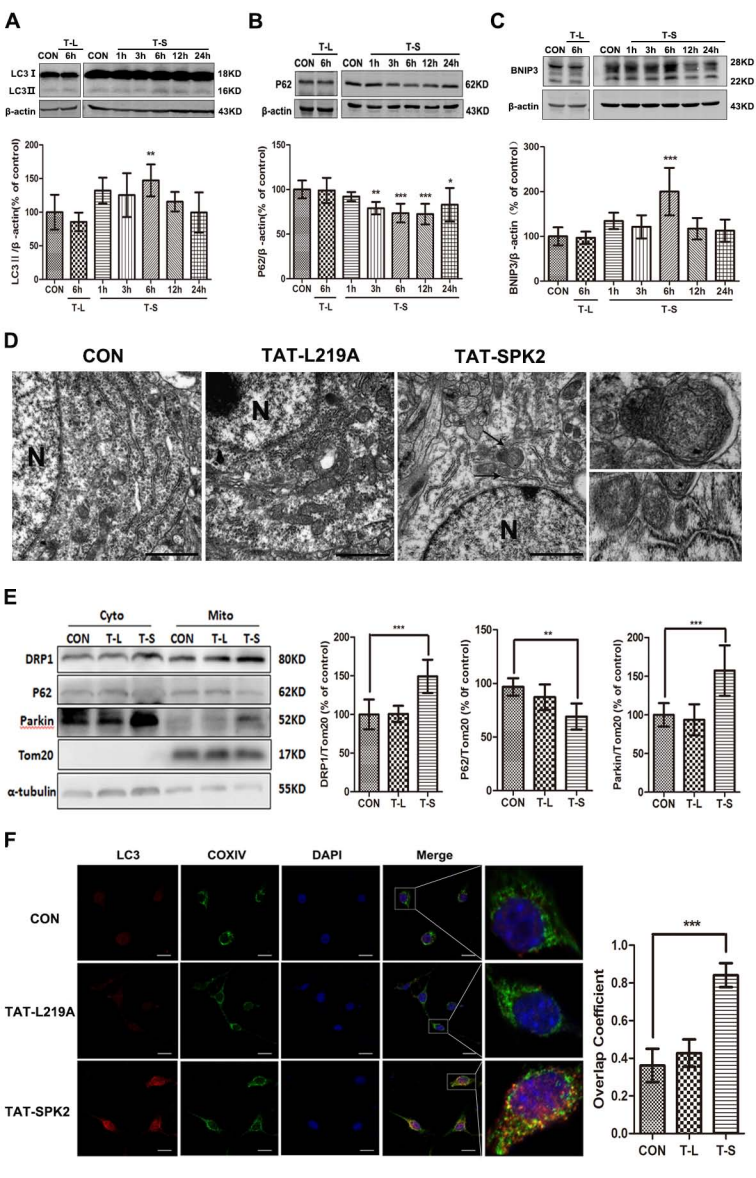
Figure 8. TAT-SPK2 peptide interacted with Bcl-2 and disrupted Beclin-1/Bcl-2 or BNIP3/Bcl-2 complex. (**A**) HT22 cells were treated with biotin-labeled peptides (10 μM, 1 h) and proteins bound to peptides were analyzed with Western blotting with anti-Bcl-2 antibody. (B-C) TAT-SPK2 reduced co-immunoprecipitation of Beclin1/Bcl-2. (D-E) TAT-SPK2 reduced co-immunoprecipitation of BNIP3/Bcl-2. HT22 cell lysates derived from vehicle- treated, TAT-L219A- treated or TAT-SPK2- treated cells were immunoprecipitated with anti-Bcl-2, separated by SDS-PAGE and subjected to Western blot analysis with the indicated antibody. β-actin levels were used as loading control. B-T-L: Biotin-TAT-L219A; B-T-S: Biotin-TAT-SPK2. n=3 independent experiments. Data were presented as mean ± SD. ** P< 0.01.

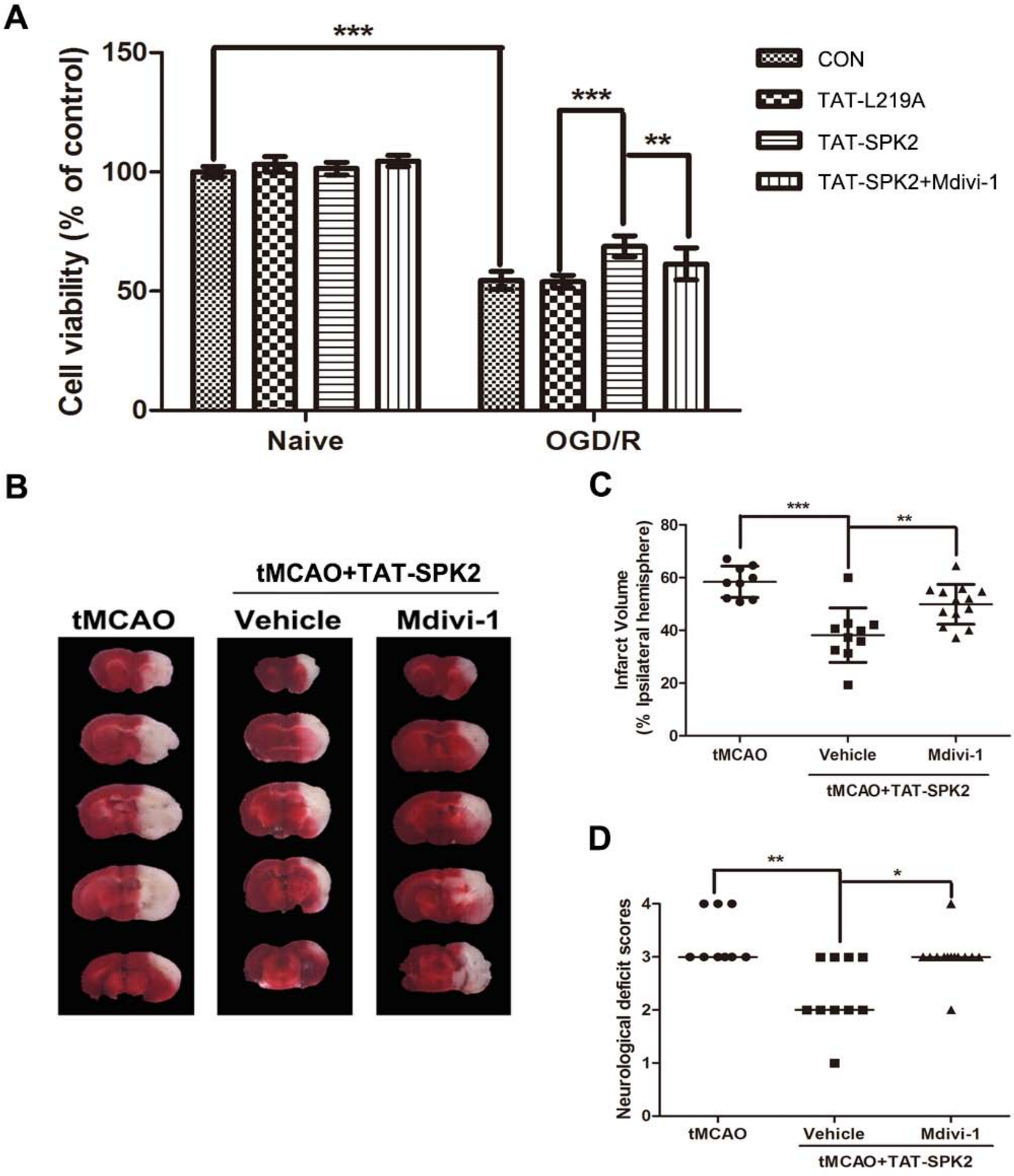

A
TAT-SPK2
Vehicle
Eda
TAT-L219A
1
2
4
(mg/kg)
Infarct Volume
(% Ipsilateral hemisphere)
80
60
40
20
0
***
***
***
Vehicle
Eda
TAT-L219A
1
2
4
(mg/kg)
TAT-SPK2
B
***
*
Neurological deficit scores
4
3
2
1
0
Vehicle
Eda
TAT-L219A
1
2
4
(mg/kg)
TAT-SPK2
C
Water content(%)
85
80
75
70
65
60
***
*
**
***
Vehicle
Eda
TAT-L219A
1
2
4
(mg/kg)
TAT-SPK2

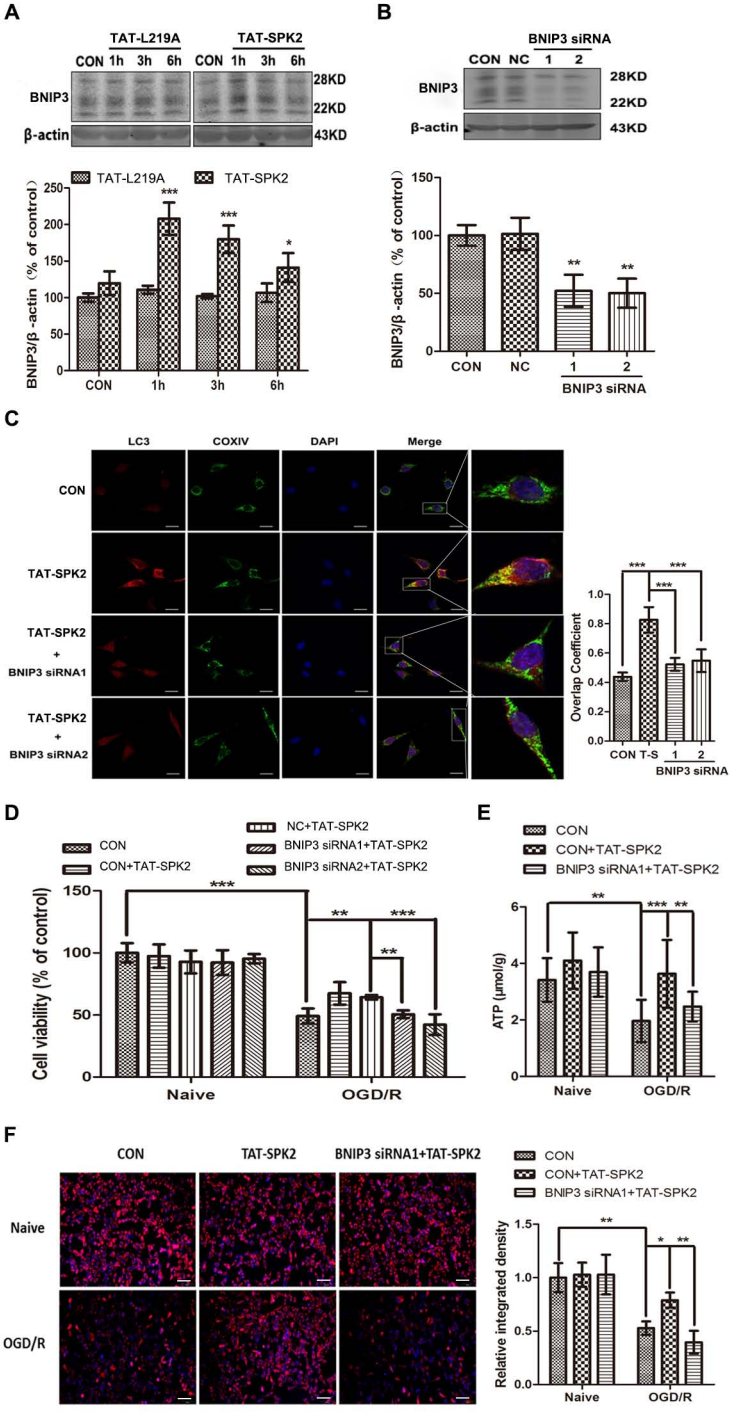

A
Vehicle
0
1
2
3
4
(h)
Reperfusion+TAT-SPK2(4mg/kg)
Infarct Volume
(% Ipsilateral hemisphere)
80
60
40
20
0
***
***
**
*
Vehicle
0
1
2
3
4
(h)
Reperfusion+TAT-SPK2(4mg/kg)
B
Neurological deficit scores
4
3
2
1
0
*
***
Vehicle
0
1
2
3
4
(h)
Reperfusion+TAT-SPK2(4mg/kg)
C
Water content(%)
90
85
80
75
70
65
60
***
**
***
**
*
Vehicle
0
1
2
3
4
(h)
Reperfusion+Tat-SPK2(4mg/kg)

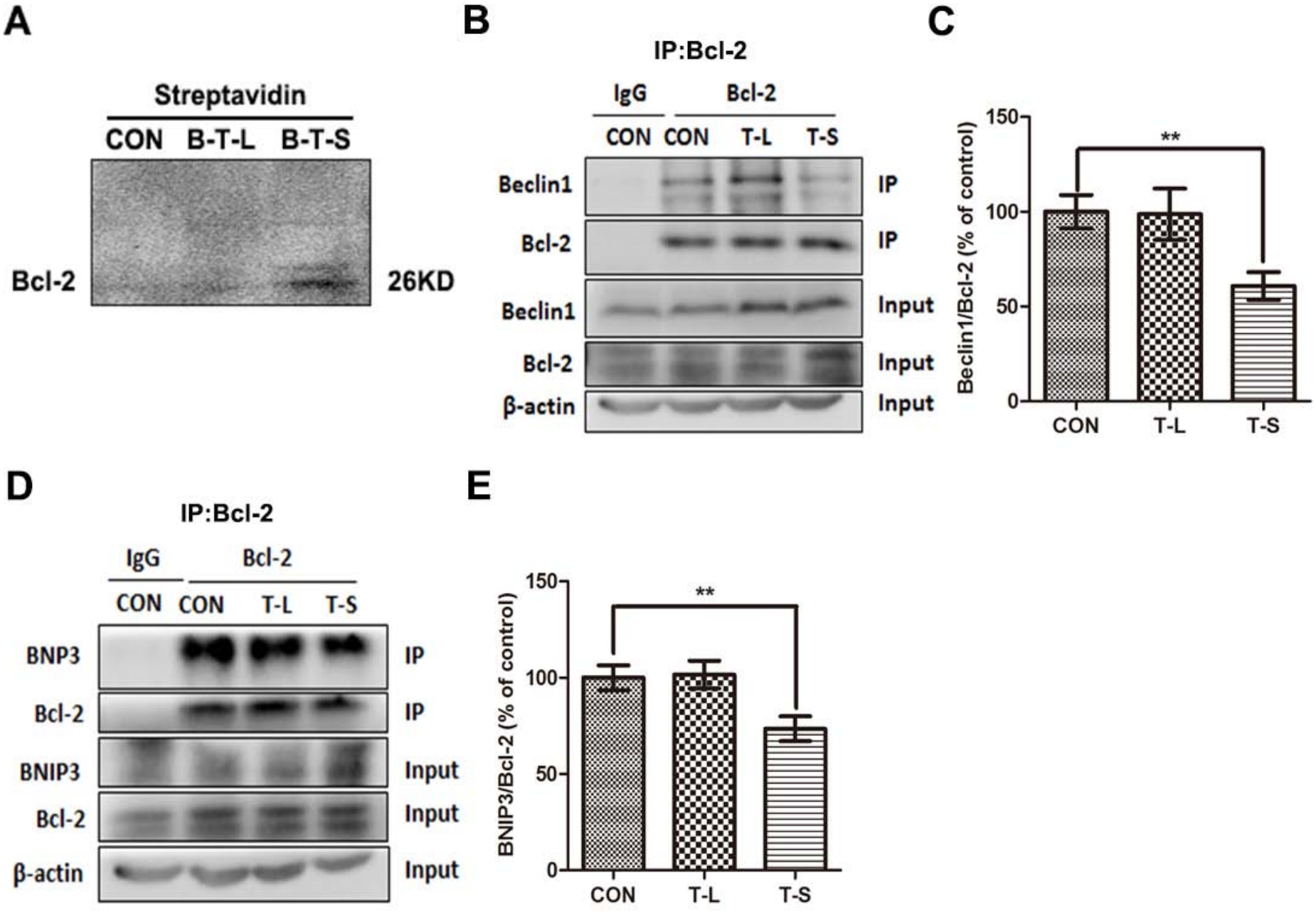

A
tMCAO
Sham
Vehicle
TAT-SPK2
Atrophy Volume
(% Ipsilateral hemisphere)
80
60
40
20
0
***
***
Sham
Vehicle
TAT-SPK2
tMCAO
B
Sham
Vehicle
TAT-SPK2
Time/cross beam
balance (seconds)
20
15
10
5
0
**
***
***
***
**
14
28
Post-ischemia (Day)
C
Sham
Vehicle
TAT-SPK2
Time/rota-rod (seconds)
400
300
200
100
0
*
***
***
***
***
14
28
Post-ischemia (Day)


A
Mean body weight (g)
35
30
25
20
1
3
5
7
9
11
13
15
17
Days
Vehicle
TAT-SPK2
B
Liver
Weight (g)
2.5
2.0
1.5
1.0
0.5
0.0
Vehicle
TAT-SPK2
C
Spleen
Weight (g)
0.20
0.15
0.10
0.05
0.00
Vehicle
TAT-SPK2
D
Kidney
Weight (g)
0.6
0.4
0.2
0.0
Vehicle
TAT-SPK2
E
Creatinine (μmol/l)
25
20
15
10
5
0
Vehicle
TAT-SPK2
F
ALT (U/l)
80
60
40
20
0
Vehicle
TAT-SPK2
G
AST (U/l)
250
200
150
100
50
0
Vehicle
TAT-SPK2
H
LDH1 (U/l)
40
30
20
10
0
Vehicle
TAT-SPK2
I
Liver
Spleen
Kidney
Testis
Heart
Lung
Vehicle
TAT-SPK2


A
T-L
T-S
CON
6h
1h
3h
6h
12h
24h
LC3Ⅰ
LC3Ⅱ
β-actin
18KD
16KD
43KD
LC3Ⅱ /β -actin(% of control)
B
P62
62KD
43KD
P62/β -actin(% of control)
C
BNIP3
28KD
22KD
43KD
BNIP3/β -actin（% of control）
D
CON
TAT-L219A
TAT-SPK2
N
E
Cyto
Mito
DRP1
P62
Parkin
Tom20
α-tubulin
80KD
62KD
52KD
17KD
55KD
DRP1/Tom20 (% of control)
P62/Tom20 (% of control)
Parkin/Tom20 (% of control)
F
LC3
COXIV
DAPI
Merge
CON
TAT-L219A
TAT-SPK2
Overlap Coefficient


A
Cell viability (% of control)
150
100
50
0
***
***
**
Naive
OGD/R
CON
TAT-L219A
TAT-SPK2
TAT-SPK2+Mdivi-1
B
tMCAO+TAT-SPK2
tMCAO
Vehicle
Mdivi-1
C
Infarct Volume
(% Ipsilateral hemisphere)
80
60
40
20
0
***
**
tMCAO
Vehicle
Mdivi-1
tMCAO+TAT-SPK2
D
Neurological deficit scores
4
3
2
1
0
**
*
tMCAO
Vehicle
Mdivi-1
tMCAO+TAT-SPK2


A
TAT-L219A
TAT-SPK2
CON 1h 3h 6h CON 1h 3h 6h
BNIP3
β-actin
28KD
22KD
43KD
TAT-L219A
TAT-SPK2
BNIP3/β -actin （% of control）
CON
1h
3h
6h
B
BNIP3 siRNA
CON NC 1 2
BNIP3
β-actin
28KD
22KD
43KD
BNIP3/β -actin （% of control）
CON
NC
1
2
BNIP3 siRNA
C
LC3
COXIV
DAPI
Merge
CON
TAT-SPK2
TAT-SPK2 + BNIP3 siRNA1
TAT-SPK2 + BNIP3 siRNA2
Overlap Coefficient
CON T-S 1 2
BNIP3 siRNA
D
CON
CON+TAT-SPK2
NC+TAT-SPK2
BNIP3 siRNA1+TAT-SPK2
BNIP3 siRNA2+TAT-SPK2
Cell viability (% of control)
Naive
OGD/R
E
CON
CON+TAT-SPK2
BNIP3 siRNA1+TAT-SPK2
ATP (μmol/g)
Naive
OGD/R
F
CON
TAT-SPK2
BNIP3 siRNA1+TAT-SPK2
Naive
OGD/R
CON
CON+TAT-SPK2
BNIP3 siRNA1+TAT-SPK2
Relative integrated density
Naive
OGD/R


A
Streptavidin
CON
B-T-L
B-T-S
Bcl-2
26KD
B
IP:Bcl-2
IgG
Bcl-2
CON
CON
T-L
T-S
Beclin1
IP
Bcl-2
IP
Beclin1
Input
Bcl-2
Input
β-actin
Input
C
Beclin1/Bcl-2 (% of control)
150
100
50
0
**
CON
T-L
T-S
D
IP:Bcl-2
IgG
Bcl-2
CON
CON
T-L
T-S
BNP3
IP
Bcl-2
IP
BNIP3
Input
Bcl-2
Input
β-actin
Input
E
BNIP3/Bcl-2 (% of control)
150
100
50
0
**
CON
T-L
T-S

Supplemental methods

Evaluation of neurological score, infarct volume and brain water content

Twenty-four hours after reperfusion, the neurological scores were measured by an investigator blinded to the experimental grouping, using the following scale (Zhou et al., 2016): Grade 0, no neurological deficit; Grade 1, failure to fully extend forelimbs when the tail was lifted; Grade 2, circling to the contralateral side; Grade 3, leaning to one side; Grade 4, no spontaneous walking, loss of consciousness. After scoring, the mice were euthanized by decapitation under anesthesia. Brains were quickly removed, cut into five 2mm slices and incubated in 1% 2,3,5-triphenyltetrazolium chloride (TTC, Sinopharm Chemical Reagent, China) at 37 ℃ for 15 min. The infarct volume was calculated using the formula: infarct volume = (red area of contralateral side – red area of ipsilateral side) / whole contralateral hemisphere area ×100% (Sheng et al., 2011). The brain slices were then dried at 105°C for 48 h until the wet weight did not change. The water content was calculated using the formula: water content = (wet weight - dried weight) / wet weight × 100% (Huang et al., 2018; Li et al., 2016).

Behavioral tests

A series of behavioral tests including beam balance test and rotarod test was conducted in a separate cohort of mice at fourteen and twenty-eight days after cerebral ischemia by two investigators blinded to the experimental grouping (Huang et al., 2018) (Li et al., 2016).

Beam balance test

The beam balance test was used to assess the balance function and motor integration. Mice were placed on a 91-cm-long and 3.5-cm-wide beam placed 57 cm above a tabletop (Li et al., 2016). Mice were trained 1 day before experiment. The time to cross the beam was recorded and the times for 3 successful runs were averaged.

Rotarod test

The rotarod test was used to assess the motor coordination of mice. A day before experiment, mice were put on a rotarod cylinder with a fixed speed of 12 rpm for training. During the next day's test, the rotarod cylinder was set to accelerate from 12 to 40 rpm within 300s. The maximum latency time of each mouse to fall from the

rotarod cylinder was recorded. Each mouse was tested three times.

In vivo peptide distribution

Mice were killed at 6h after administration of 4 mg/kg biotin-TAT-SPK2 or biotin-SPK2. Brains were perfused with PBS, fixed in 4% paraformaldehyde, cryopreserved with 20% and 30% sucrose at 4℃, and kept frozen at -20℃ overnight. Brains were cut into 20-μm-thick sections with a cryostat. Sections were blocked in 5% BSA, 0.4% Triton X-100 for 1h, and then incubated with Alexa Fluor 488-conjugated streptavidin (1:500; Vector Laboratories BA-2000) for 1 h (Liu et al., 2013b). Fluorescence images were captured using a laser confocal microscope (ZEISS LSM710).

Toxicology assessment

In the acute toxicity study, normal mice were administered intraperitoneally with a single dose of 80 mg/kg TAT-SPK2 (20 times the highest therapeutic dose) or TAT-L219A (6 mice per group). Mice were monitored for body weight, food and water intake, breathing, excretion and behavior 3 times within 24 hours after administration, and once a day thereafter for another 6 days. In the subacute toxicity study, normal mice received vehicle or TAT-SPK2 (4 mg/kg/day, intraperitoneal injection) for 2 weeks (6 mice per group). Mice were observed daily for weight, food and water intake, breathing, excretion and behavior during the administration.

On the last day of toxicity assessment, the blood of the mice was collected under anesthesia. The blood was placed at room temperature for 2 h, and was centrifuged at 3000 rpm for 20 min at 4℃ to obtain serum. The creatinine, glutamic pyruvic transaminase (GPT, alanine aminotransferase, ALT), glutamic oxalacetic transaminase (GOT, aspartate aminotransferase, AST) and lactate dehydrogenase 1 (LDH1) in serum were analyzed. The mice were sacrificed under anesthesia, and the organs including heart, lung liver, kidney, spleen and testis were removed. The samples stored in 10% buffered formalin were dehydrated through a series of graded alcohols, embedded in paraffin, sliced into 5 μm thick sections and stained with hematoxylin-eosin for pathological examination (Shen et al., 2015).

Figure S1. Experimental design of in vivo (A) and in vitro studies (B). (A) The in vivo studies sought to examine the effects of TAT-SPK2 on ischemia reperfusion injury and BNIP3-mediated mitophagy in a mouse tMCAO model. In the short term study, we performed peptide entry assay, efficacy, time window and mitophagy assay. In long term study, we investigated the effect of TAT-SPK2 on ischemic atrophy and long-term functional recovery. Finally, we evaluated the preliminary toxicity of TAT-SPK2. (B) In vitro studies were aimed at exploring the role and mechanism of BNIP3-mediated mitophagy in the neuroprotection of TAT-SPK2, and included mitophagy assay and protein interaction between BNIP3/Beclin1 and Bcl-2.

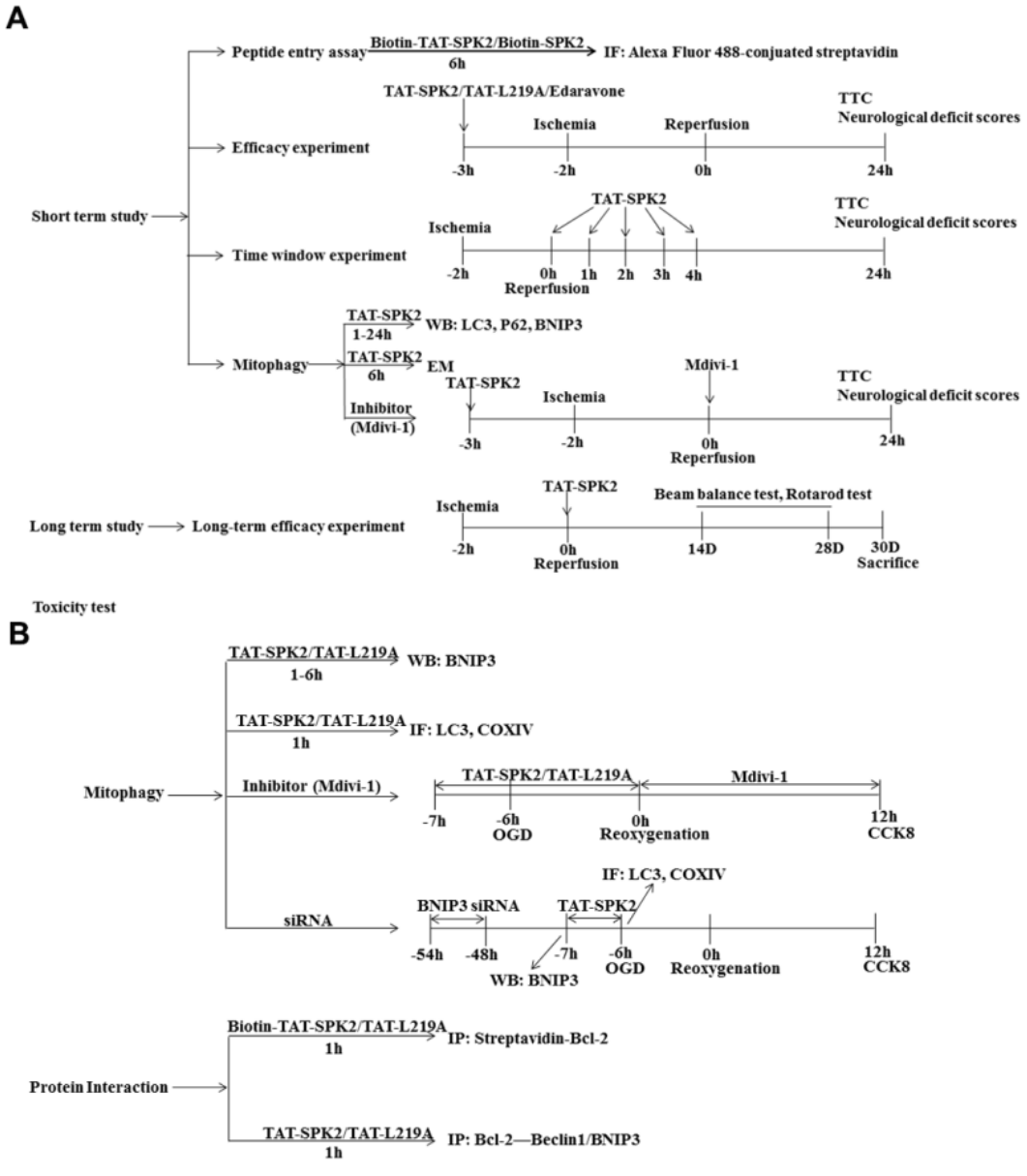


Figure S2. Intracellular staining of biotin-Tat-SPK2 peptide in the brain.

Six hours after treatment with Biotin-Tat-SPK2 or Biotin-SPK2 peptide (4 mg/kg, intraperitoneally) , mice were perfused with PBS, fixed in 4% paraformaldehyde, and dehydrated with 20% and 30% sucrose. After frozen overnight, the brain was cut into 20-μm-thick sections and processed for immunofluorescence. Biotin was detected by Alexa Fluor 488 conjugated streptavidin (green). Scale bar=20 μm. n=3 mice.

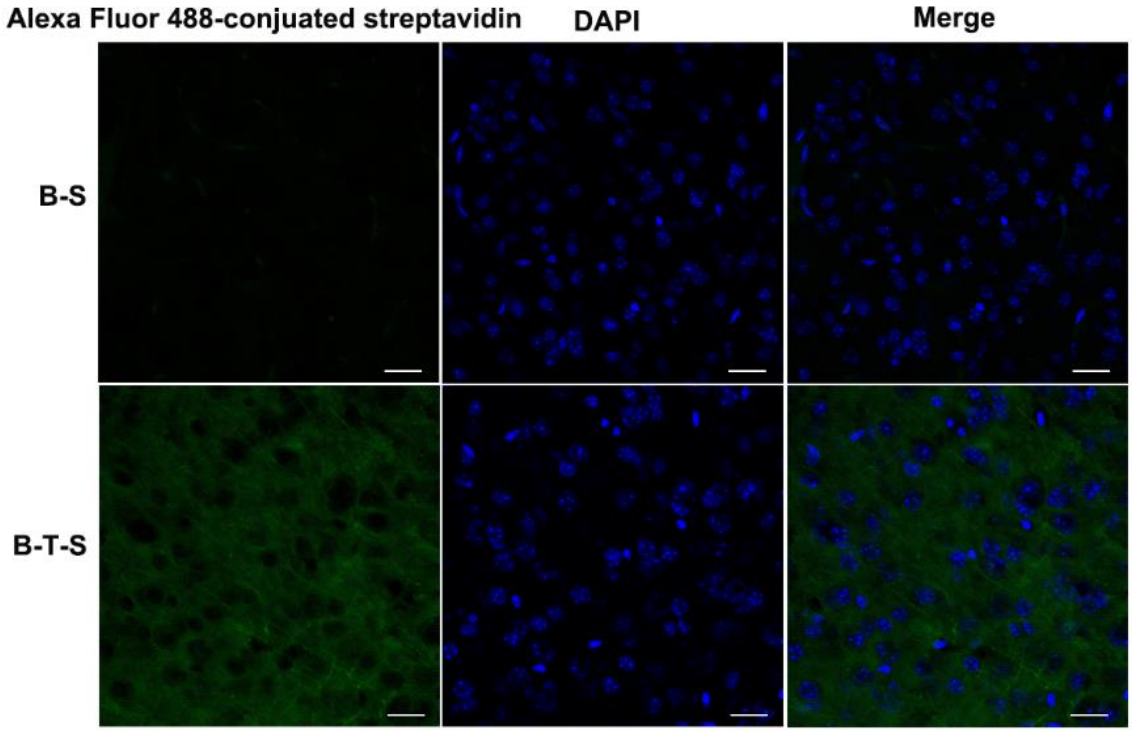


Figure S3. Preliminary toxicological evaluation of TAT-SPK2 in mice. Normal mice were administered intraperitoneally with a single dose of 80 mg/ kg of TAT-SPK2 (20 times the highest therapeutic dose) or TAT-L219A. (A) The effects of TAT-SPK2 on body weights were assessed. Some representative objective blood biomarkers of organs toxicity were tested including creatinine (E) for kidney, glutamic pyruvic transaminase (GPT, alanine aminotransferase, ALT) (F) and glutamic oxalacetic transaminase (GOT, aspartate aminotransferase, AST) (G) for liver, and lactate dehydrogenase 1 (LDH1) for heart (H). Organs including liver, spleen, kidney, testis, heart and lung were dissected and stained with haematoxylin and eosin. Representative images are shown. Scale bar = 50 μm. n=6 mice in each group. Data are shown as mean ± SD.

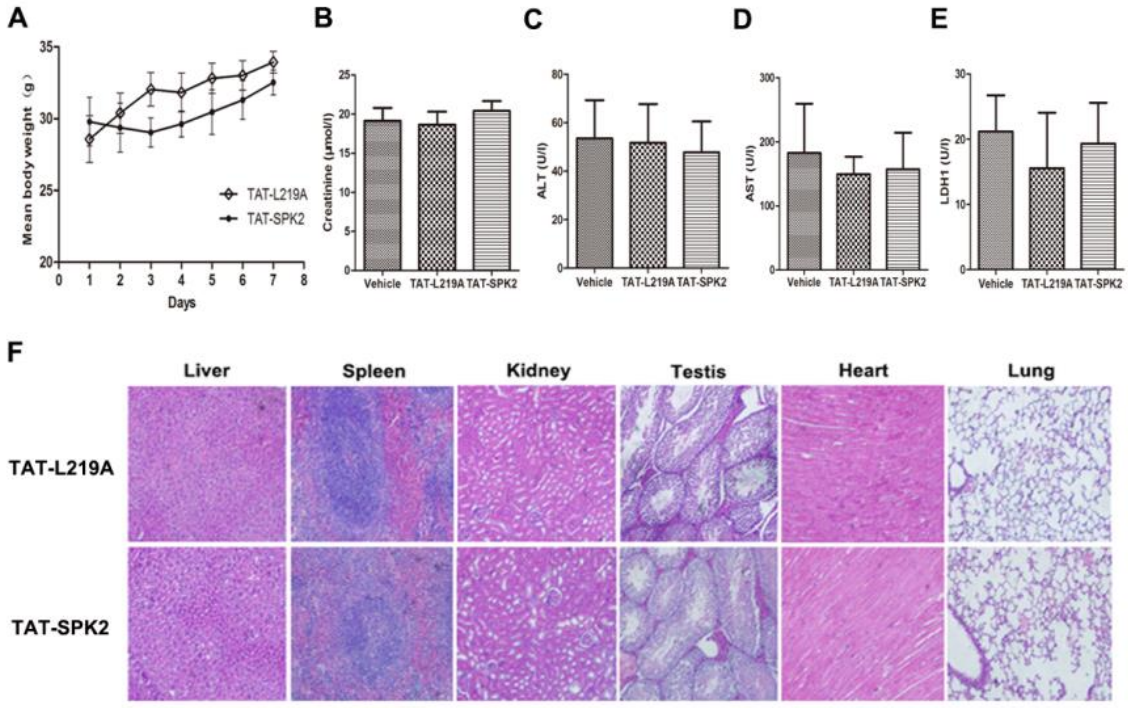


Figure S4. Tat-SPK2 peptide upregulates LC3II and downregulates P62 in the hippocampus and striatum of mice. Mice were treated with Tat-SPK2 peptide or Tat-L219A (4mg/kg, intraperitoneally). Hippocampus and striatum were dissected at 1, 3, 6, 12, and 24h after administration. The levels of LC3 (A) and P62 (B) were determined by Western blotting. β-actin levels were used as loading control. n=6 mice. Data are shown as mean ± SD. * P<0.05, ** P< 0.01, *** P<0.001 compared with the control group.

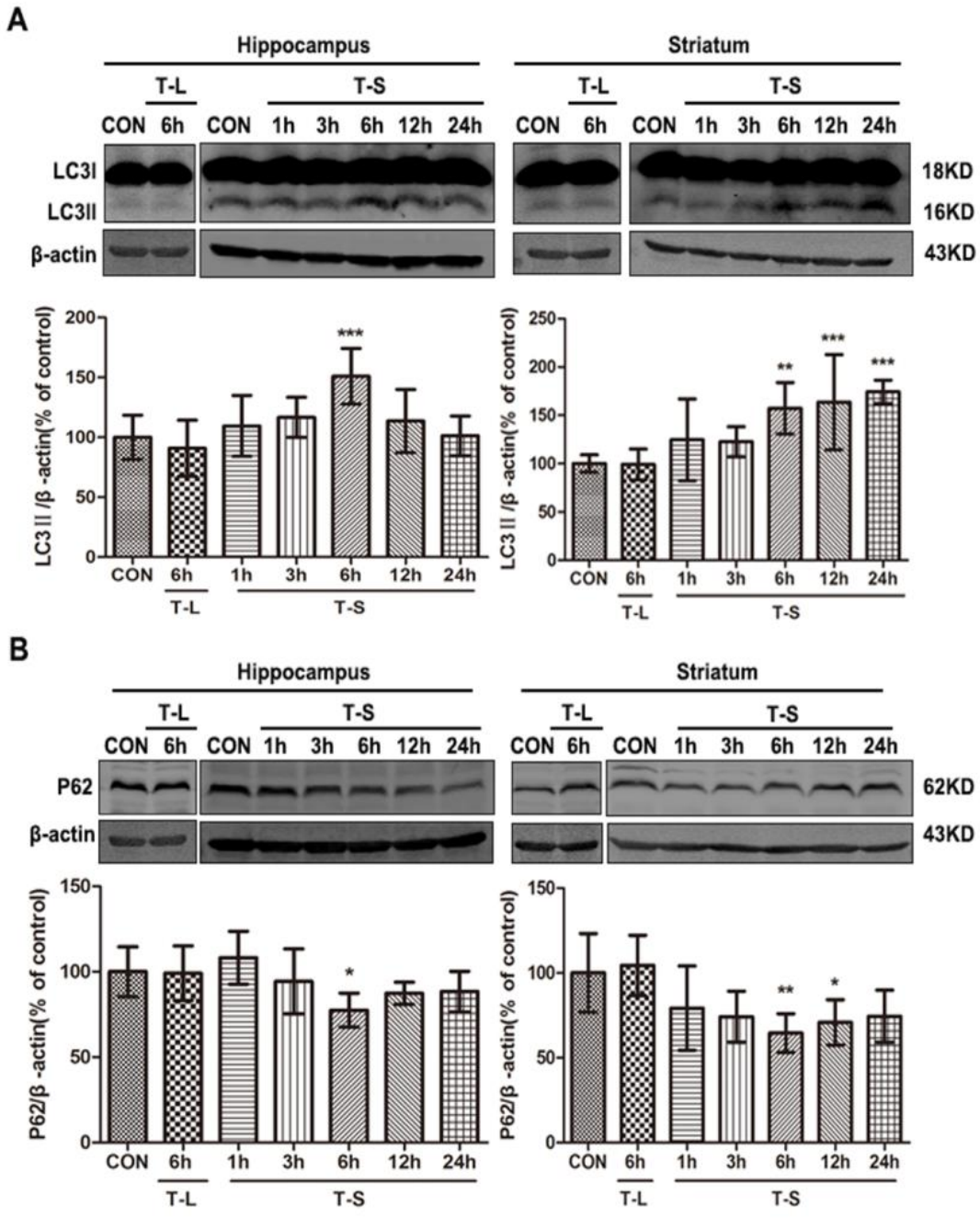
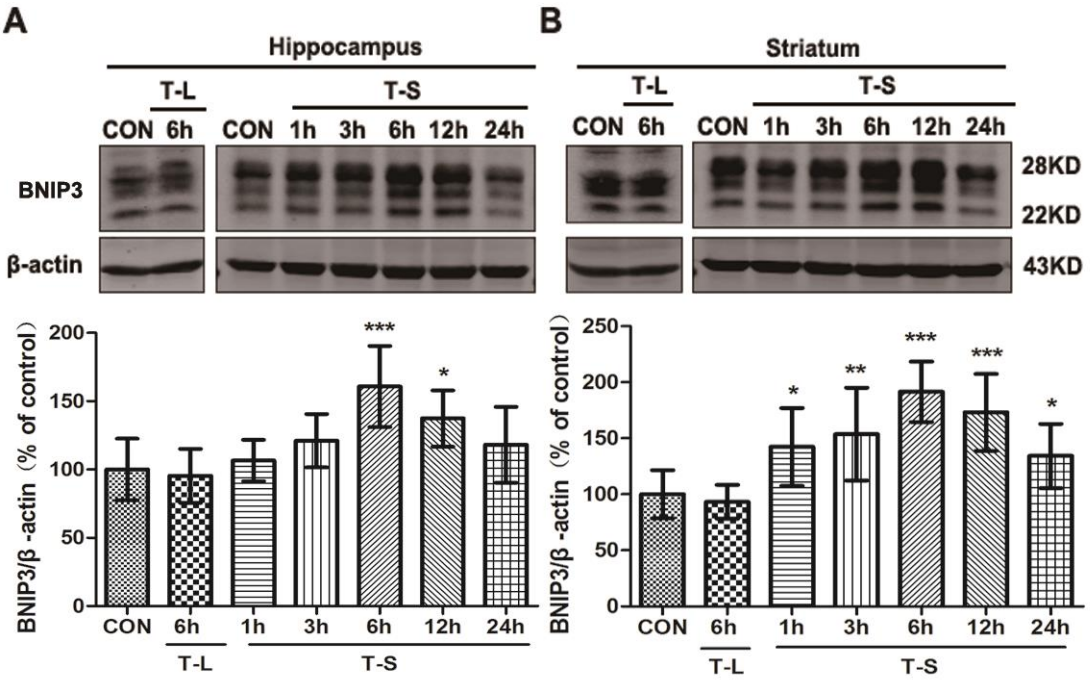


Figure S5. Tat-SPK2 peptide upregulates BNIP3 in the hippocampus and striatum of mice. Mice were treated with Tat-SPK2 peptide or Tat-L219A (4mg/kg, intraperitoneally). Hippocampus and striatum were dissected at 1, 3, 6, 12, and 24h after administration. BNIP3 level was determined by Western blotting. β-actin levels were used as loading control. n=6 mice. * P<0.05, ** P< 0.01, *** P<0.001 compared with the control group.



Supplemental Table 1: Total number and group allocation of mice subjected to transient middle cerebral artery occlusion (tMCAO).

Group	Total number of mice	Excluded mice		Mice included in analysis
		Death (during surgery or within 24-hour unless noted otherwise)	Technical failure (blood flow not reduced by 90% during MCAO or not recovered to 85-95% of baseline during reperfusion)	
Vehicle	14	3	1	10
Eda	13	1	3	9
TAT-L219A	13	2	0	11
TAT-SPK2 1mg/kg	13	1	0	12
TAT-SPK2 2mg/kg	13	1	1	11
TAT-SPK2 4mg/kg	13	0	2	11
Vehicle	12	1	2	9
TAT-SPK2 0h	12	0	4	8
TAT-SPK2 1h	13	2	0	11
TAT-SPK2 2h	12	1	2	9
TAT-SPK2 3h	12	0	2	10
TAT-SPK2 4h	12	2	0	10
tMCAO+Vehicle	38	1-24h; 20-1 week; 8-2 week	3	6
tMCAO+TAT-SPK2	26	2-24h; 10-1 week; 6-2 week	2	6
tMCAO	12	0	3	9
tMCAO+TAT-SPK2+Vehicle	12	1	1	10
tMCAO+TAT-SPK2+Mdivi-1	14	1	0	13